

T-3228

**ERROR ANALYSIS AND DESIGN CONSIDERATIONS  
FOR BACKPRESSURE TESTING OF GAS WELLS**

By

S. B. Hinchman

**ARTHUR LAKES LIBRARY  
COLORADO SCHOOL of MINES  
GOLDEN, COLORADO 80401**

ProQuest Number: 10782813

All rights reserved

INFORMATION TO ALL USERS

The quality of this reproduction is dependent upon the quality of the copy submitted.

In the unlikely event that the author did not send a complete manuscript and there are missing pages, these will be noted. Also, if material had to be removed, a note will indicate the deletion.



ProQuest 10782813

Published by ProQuest LLC (2018). Copyright of the Dissertation is held by the Author.

All rights reserved.

This work is protected against unauthorized copying under Title 17, United States Code  
Microform Edition © ProQuest LLC.

ProQuest LLC.  
789 East Eisenhower Parkway  
P.O. Box 1346  
Ann Arbor, MI 48106 – 1346

T-3228

A thesis submitted to the Faculty and the Board of Trustees of the Colorado School of Mines in partial fulfillment of the requirements for the degree of Master of Science, Petroleum Engineering.

Golden, Colorado

Date 4-10-87

Signed: Steven B. Hinchman

Steven B. Hinchman

Approved: Fred H. Poettmann

Dr. Fred H. Poettmann  
Thesis Advisor

Golden, Colorado

Date April 15, 1987

Craig W. Van Kirk

Dr. Craig W. Van Kirk  
Head, Department of  
Petroleum Engineering

**ABSTRACT**

The theoretical validity of backpressure tests has been analyzed for wells in radial flow and for wells intersected by vertical fractures. It is demonstrated that stabilized flow-after-flow and isochronal tests are valid tests. Unstabilized flow-after-flow and modified isochronal tests result in error in predicted deliverability caused by continued influence of prior flow and shut-in periods (superposition error). It is shown how the superposition error can be minimized by proper selection and design of the backpressure test.

Isochronal and modified isochronal tests are unsteady-state methods and provide the transient deliverability of a well. An extended flow period is generally used to determine the stabilized deliverability. In many reservoirs extended flow periods are unreasonably expensive and impractical. Analytical solutions for predicting stabilized deliverability are required. The calculations generally used in the prediction of stabilized gas deliverability are based on a radial flow geometry. When these calculations are applied to other flow geometries, erroneous predictions of stabilized deliverability result. In this study a fully-implicit, two-dimensional gas simulator was used to

demonstrate the extension of radial flow theory to vertically fractured gas wells. The effect of fracture length and conductivity was investigated under Darcy flow. It was demonstrated that the flow exponent was not sensitive to fracture conductivity or length. However, the performance coefficient was dependent upon time, fracture length, and conductivity.

A linear or radial assumption for flow in a well intersected by a finite conductivity vertical fracture will result in an erroneous stabilized performance coefficient, thus an erroneous Absolute Open Flow (AOF).

The performance coefficient is inversely related to pressure behavior with time. Linear flow can be determined by plotting  $(1/C_t)^{1/n}$  vs time on log-log paper and observing a half slope. For radial flow a plot of  $(1/C_t)^{1/n}$  vs log time will provide a line with constant slope which can be used to estimate reservoir properties and extrapolated to a stabilized value.

Wellbore storage (WBS) will cause the AOF to be overestimated. Wells producing with large drawdown will result in erroneous deliverability if flow periods do not last longer than the influence of WBS.

TABLE OF CONTENTS

ABSTRACT . . . . .	iii
LIST OF FIGURES . . . . .	vi
LIST OF TABLES . . . . .	x
ACKNOWLEDGMENTS . . . . .	xi
INTRODUCTION . . . . .	1
REVIEW OF PERTINENT LITERATURE . . . . .	4
BACK PRESSURE TEST VALIDITY . . . . .	16
Flow-After-Flow . . . . .	16
Isochronal . . . . .	19
Modified Isochronal . . . . .	23
DELIVERABILITY OF VERTICALLY FRACTURED WELLS . . . . .	32
GENERALIZED STABILIZED DELIVERABILITY . . . . .	56
EFFECT OF WELLBORE STORAGE ON BACKPRESSURE TESTS . . . . .	64
CONCLUSIONS . . . . .	67
RECOMMENDATIONS FOR FUTURE RESEARCH . . . . .	70
NOMENCLATURE . . . . .	71
REFERENCES . . . . .	74
APPENDICES . . . . .	81
A. Derivation of Superposition Error . . . . .	81
B. Derivation of Dimensionless Backpressure Expression . . . . .	88

TABLE OF CONTENTS

C. Derivation of  $(1/C)^{1/n}$  Relationship  
With Time . . . . . 90

LIST OF FIGURES

1.	Flow-After-Flow Test . . . . .	5
2.	Isochronal Test . . . . .	8
3.	Modified Isochronal Test . . . . .	9
4.	Backpressure Curve for a Flow-After-Flow Test and Isochronal Test . . . . .	11
5.	Normalized Backpressure Curve . . . . .	13
6.	Absolute Error in "n" - Flow-After-Flow Test . . .	21
7.	Absolute Error in "n" - Modified Isochronal Test . . . . .	27
8.	Comparison of Error Between an Unstablized Flow-After-Flow Test and Modified Isochronal Test . . . . .	28
9.	Absolute Error in "n" for Flow Time To Shut-In Time Ratio Less Than One - Modified Isochronal Test . . . . .	29
10.	Comparison of Numerical Simulator to Line Source Solution . . . . .	33
11.	Comparison of Numerical Simulator to Analytical Solution for Infinite Conductivity Vertical Fractures in Bounded Systems . . . . .	34
12.	Comparison of Numerical Simulator to Analytical Solution for Finite Conductivity Vertical Fractures . . . . .	36
13.	Simulated Isochronal Test, Radial Flow . . . . .	37
14.	Simulated Isochronal Test, Finite Conductivity Vertical Fracture ( $F_{CD} = 0.1 X_f = 10$ ft) . . . .	38
15.	Simulated Isochronal Test, Finite Conductivity Vertical Fracture ( $F_{CD} = 0.1 X_f = 100$ ft) . . . .	39

LIST OF FIGURES

16.	Simulated Isochronal Test, Finite Conductivity Vertical Fracture ( $F_{CD} = 0.1$ $X_f = 1000$ ft) . . . .	40
17.	Simulated Isochronal Test, Finite Conductivity Vertical Fracture ( $F_{CD} = 1.0$ $X_f = 10$ ft) . . . .	41
18.	Simulated Isochronal Test, Finite Conductivity Vertical Fracture ( $F_{CD} = 1.0$ $X_f = 100$ ft). . . .	42
19.	Simulated Isochronal Test, Finite Conductivity Vertical Fracture ( $F_{CD} = 1.0$ $X_f = 1000$ ft) . . . .	43
20.	Simulated Isochronal Test, Finite Conductivity Vertical Fracture ( $F_{CD} = 10$ $X_f = 10$ ft). . . .	44
21.	Simulated Isochronal Test, Finite Conductivity Vertical Fracture ( $F_{CD} = 10$ $X_f = 100$ ft) . . . .	45
22.	Simulated Isochronal Test, Finite Conductivity Vertical Fracture ( $F_{CD} = 10$ $X_f = 1000$ ft). . . .	46
23.	Simulated Isochronal Test, Finite Conductivity Vertical Fracture ( $F_{CD} = 100$ $X_f = 10$ ft) . . . .	47
24.	Simulated Isochronal Test, Finite Conductivity Vertical Fracture ( $F_{CD} = 100$ $X_f = 100$ ft). . . .	48
25.	Simulated Isochronal Test, Finite Conductivity Vertical Fracture ( $F_{CD} = 100$ $X_f = 1000$ ft) . . . .	49
26.	Dimensionless Performance Coefficient for a Finite Conductivity Vertically Fractured Gas Well . . . . .	50
27.	Radial Flow Extrapolation to Determine the Stabilized Performance Coefficient for a Finite Conductivity Vertically Fractured Gas Well . . . .	51
28.	Linear Flow Extrapolation to Determine the Stabilized Performance Coefficient for a Finite Conductivity Vertically Fractured Gas Well . . . .	52

LIST OF FIGURES

29. Time to Pseudo-Radial Flow for a Finite  
Conductivity Vertically Fractured Gas Well . . . . 53

30. Linear Flow/Radial Flow Extrapolation to  
Determine the Stabilized Performance Coeffi-  
cient for a Finite Conductivity Vertically  
Fractured Gas Well . . . . . 54

31. Comparison of  $1/C_{tD}$  and  $P_D$  for a Finite  
Conductivity Vertically Fractured Gas Well . . . . 58

32. Stabilized Performance Coefficient for a  
Finite Conductivity Vertically Fractured  
Gas Well . . . . . 60

33.  $(1/C_t)^{1/n}$  vs Log Time (Cullender) . . . . . 63

LIST OF TABLES

1. Base Case Parameters . . . . . 20

2. Sensitivity of Error in "n" to Flow Rate Ratio  
and Sequence - Flow-After-Flow Test . . . . . 22

3. Sensitivity of Error in "n" to Flow Rate Ratio  
and Sequence - Modified Isochronal Test . . . . . 30

ACKNOWLEDGMENTS

The author wishes to express his special gratitude and sincere appreciation to Dr. Fred H. Poettmann of Colorado School of Mines for his supervision and cooperation throughout this study. Sincere appreciation is also expressed to Marathon Oil Company for use of the numerical simulator and computing time. Many thanks are also due to Carolyn Cain for her help in typing this manuscript. Finally, I would like to express my appreciation for the understanding and support of my wife, Peggy, throughout the preparation of this work.

## INTRODUCTION

Gas well deliverability tests are multirate tests consisting of three or more flows with pressures, rates and other data being recorded as a function of time. These tests are usually required by state regulatory agencies for proration purposes and to obtain an allowable. In addition, these tests can provide information for performing reservoir and production engineering studies such as production forecasting, field development, sizing of gathering and trunk lines, evaluating skin damage, and establishing a base performance curve for future comparison.

Basically, there are two different types of deliverability tests: (1) flow after flow test, and (2) Isochronal tests. The flow after flow test consists of a series of increasing flow rates (normal sequence) or decreasing flow rates (reverse sequence) on a well starting from an initial shut-in condition, with no shut-in periods between rate changes. This type of test is valid only if the well has "stabilized" during each flow period. Flowing times are arbitrary or can be set by regulatory bodies. The Isochronal method involves a series of flowing and shut-in periods. Each flow period starts after a shut-in period which has reached the "static condition". As a result, any

pressure rise occurring due to shut-in will not affect pressure during the subsequent flow. An isochronal test, as the name implies, is based on equal flow periods so that the drainage radius established during each flow period is repeated.

The first objective of this investigation is to determine the validity of backpressure testing and to quantify any error. As a result, backpressure test design considerations have been developed.

Analysis of backpressure testing is based on the assumption that flow is radial. However, in many instances, particularly in low permeability wells, stimulation in the form of hydraulic fracturing or acid fracturing is required for wells to be commercial. In such cases flow is likely to be linear, transitional, and radial during the testing period. The second objective of investigation is to examine the applicability of commonly accepted solutions on estimating stabilized deliverability of fractured gas wells. The effect of fracture conductivity and length has been investigated.

With the advent of deeper drilling, gas wells drain reservoirs with very low permeability. In such cases, wellbore storage (WBS) can control flow behavior for a

substantial period of time. The third objective is to evaluate the effect of WBS on backpressure tests.

### REVIEW OF PERTINENT LITERATURE

Backpressure tests are multiple rate transient tests consisting of three or more flow periods (1,2,3,4,5,6). These tests are generally required by state regulatory agencies for proration purposes and establishing allowables (7). Additionally, the tests can provide reservoir and completion information (8,9,10).

There are two types of backpressure tests: 1) flow-after-flow, and 2) isochronal. In 1936, Rawlins and Schellhardt introduced the concept of backpressure testing using the flow-after-flow test (1). The flow-after-flow test starts from a stabilized shut-in condition after which a series of increasing (normal) or decreasing (reverse) flow periods are imposed. The flow rate and pressure response are shown in Figure 1. No shut-in period occurs between flows, and the flow periods should be of sufficient duration to reach Pseudosteady-state (or stabilized flow). Failure to obtain the stabilized flow condition will result in an erroneous deliverability prediction. Stabilized flow is normally achieved only in high permeability reservoirs.

Cullender presented the isochronal test as an empirical method in 1955 (2). The isochronal test was designed for use in those wells which do not stabilize in a relatively short period of time. The isochronal test requires

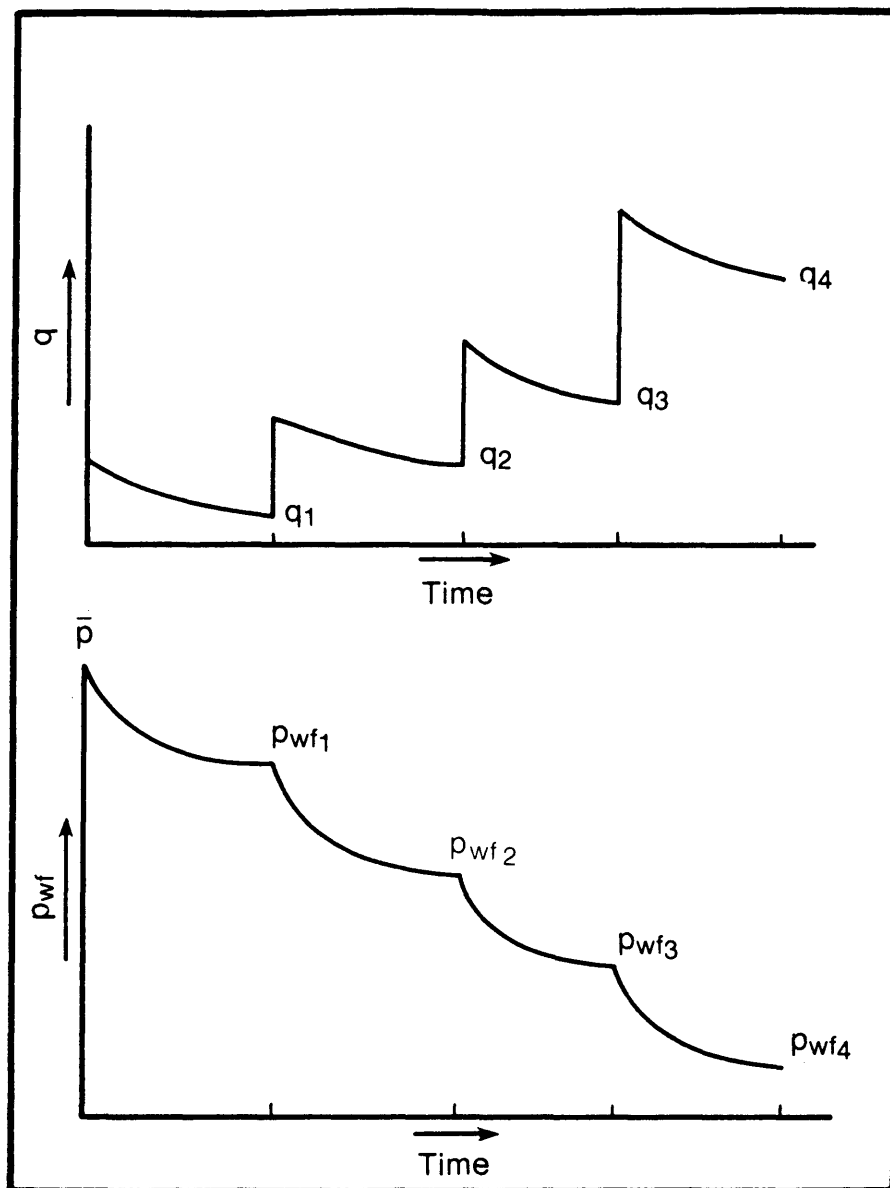


Figure 1. Flow-After-Flow Test

that each flow period begin from a static reservoir condition, thus the shut-in periods are of sufficient duration to reach the static reservoir pressure. The flow rate and pressure response for an isochronal test are shown in Figure 2. A common misconception in isochronal testing of gas wells is that a well must be tested at constant flow rate. This is seldom possible since gas wells are normally tested by opening them on a fixed choke size which will lead to decreasing rates and pressures with time. It is important that one does not use an average rate for each flow period -- the flow rate corresponding to the time at which the pressure is being evaluated should be used. The isochronal test provides a transient deliverability; for stabilized deliverability an extended flow period or an analytical method for its prediction is needed.

In low permeability gas reservoirs it may require days to reach stabilized pressure during the shut-in period of an isochronal test, even after relatively short flow periods. To shorten the test duration a modification of the isochronal test was introduced. The modified isochronal test does not achieve stabilized pressure during the shut-in periods. It is typically run with equal flow and shut-in periods. Depiction of such a case is shown in Figure 3. The modified isochronal test will have error caused by the

unstabilized flow and shut-in periods (11,12). Additionally, the modified isochronal test produces transient deliverability.

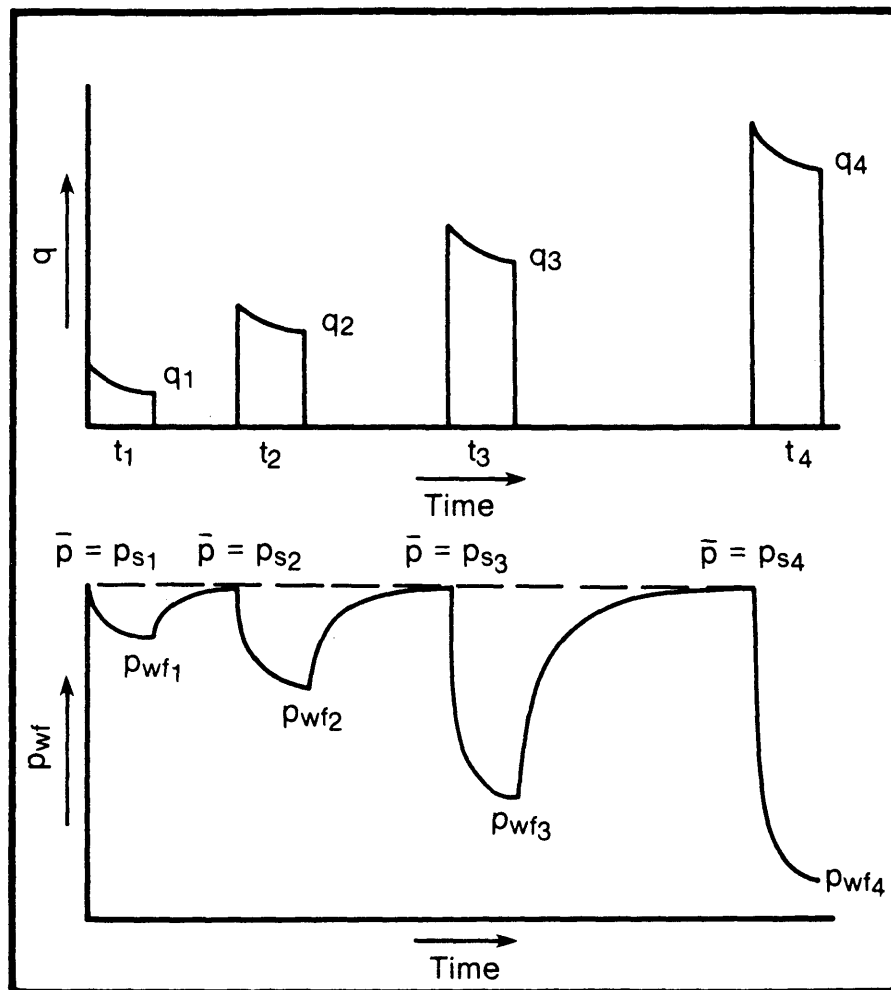


Figure 2. Isochronal Test

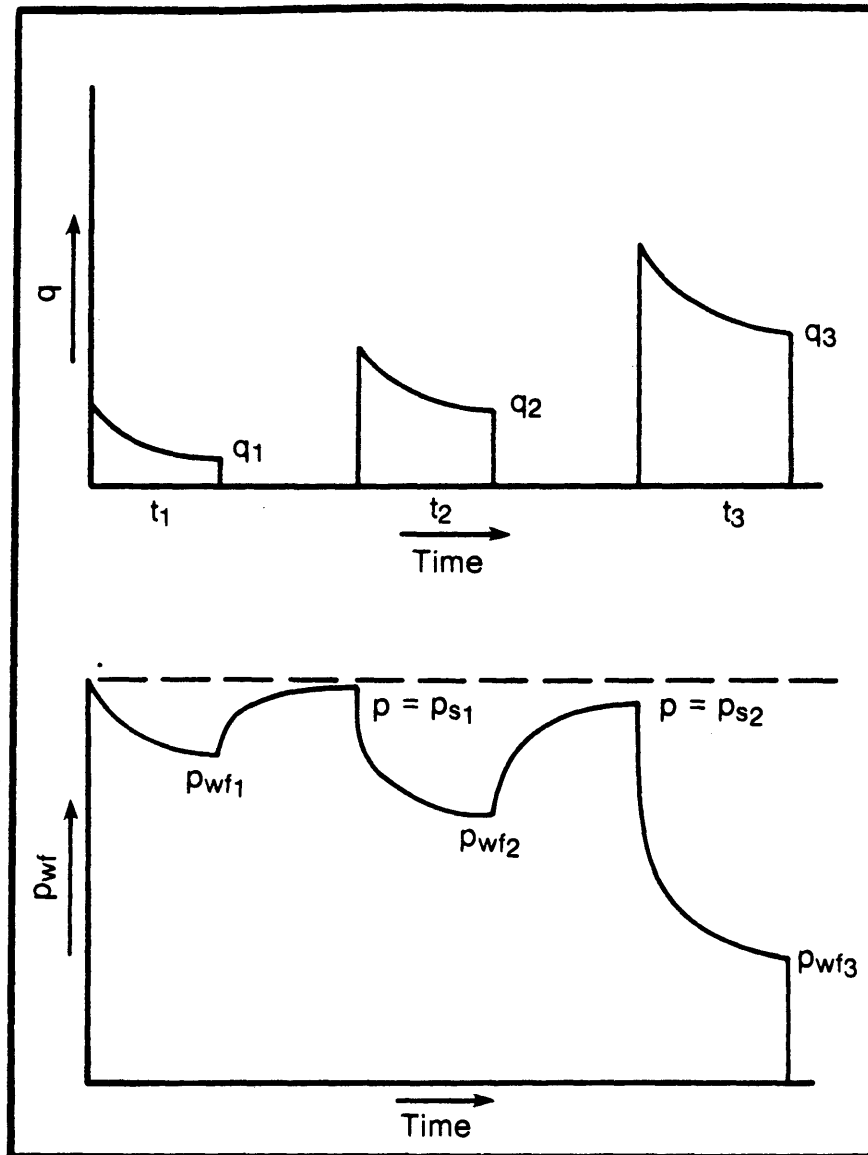


Figure 3. Modified Isochronal Test

Gas deliverability is generally determined by use of the Rawlins and Schellhardt backpressure expression (1):

$$q_{SC} = C_S (\bar{P}_R^2 - P_{wf}^2)^n \quad (1)$$

where  $C_S$  is the stabilized performance coefficient, and "n" is the flow exponent. The transient performance coefficient ( $C_t$ ) depends on physical properties of the reservoir (rock and fluid) and time. The flow exponent "n" is an empirical adjustment enabling Equation (1) to describe, over a limited flow rate range, non-Darcy flow. The flow exponent "n" can physically vary between 1, for Darcy flow, and approach 0.5, for dominantly non-Darcy flow. A 0.5 flow exponent is impossible since it requires having non-Darcy flow throughout the entire drainage radius. If the gas flow rate is plotted on log-log graph paper vs the respective difference of the square of the static or shut-in reservoir pressure and flowing sandface pressure, the relationship is represented as a straight line shown in Figure 4 and is referred to as a performance plot. The performance coefficient is determined by extrapolating the line to a  $\Delta P^2$  value of one. The performance coefficient is then read directly from the flow rate axis. The slope of the line is the inverse of the flow exponent.

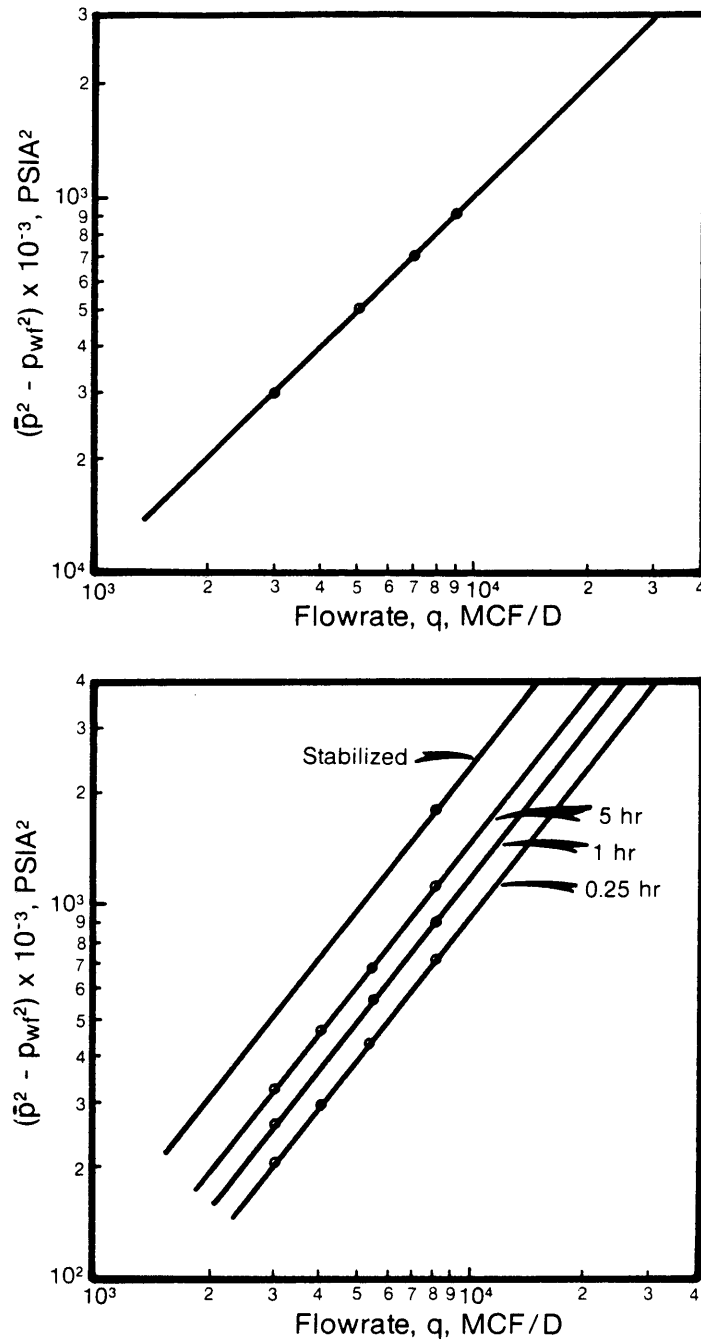


Figure 4. Backpressure Curve for a Flow-After-Flow Test and Isochronal Test

The Forchheimer equation more rigorously accounts for non-Darcy flow (13,14,15):

$$P_R - p_{wf}^2 = a q_{sc} + b q_{sc}^2 \quad (2)$$

The first term of the Equation (2) ( $aq_{sc}$ ) is the Darcy flow term and is a function of time during the transient flow period. The second term ( $bq_{sc}^2$ ) is the non-Darcy flow term and is independent of time. Several orders of magnitude change in the flow rate is necessary to cause an observable change in slope. This is illustrated in a normalized performance plot generated using Equation (2) and shown in Figure 5 (16). Since flow rates generally vary only over one order of magnitude, the Rawlins and Schellhardt backpressure expression remains a practical alternative to the Forchheimer equation. Figure 5 also suggests that non-Darcy dominance is unlikely for reservoir flow, and that the rate sensitive pressure drop is more likely to occur through the well completion.

Cornell recognized that the unstabilized performance coefficient ( $C_t$ ) is a function of time for transient flow (17). Numerous studies have furnished techniques for determining the stabilized deliverability (18,19,20,21,22,23, 24,25,26,27).

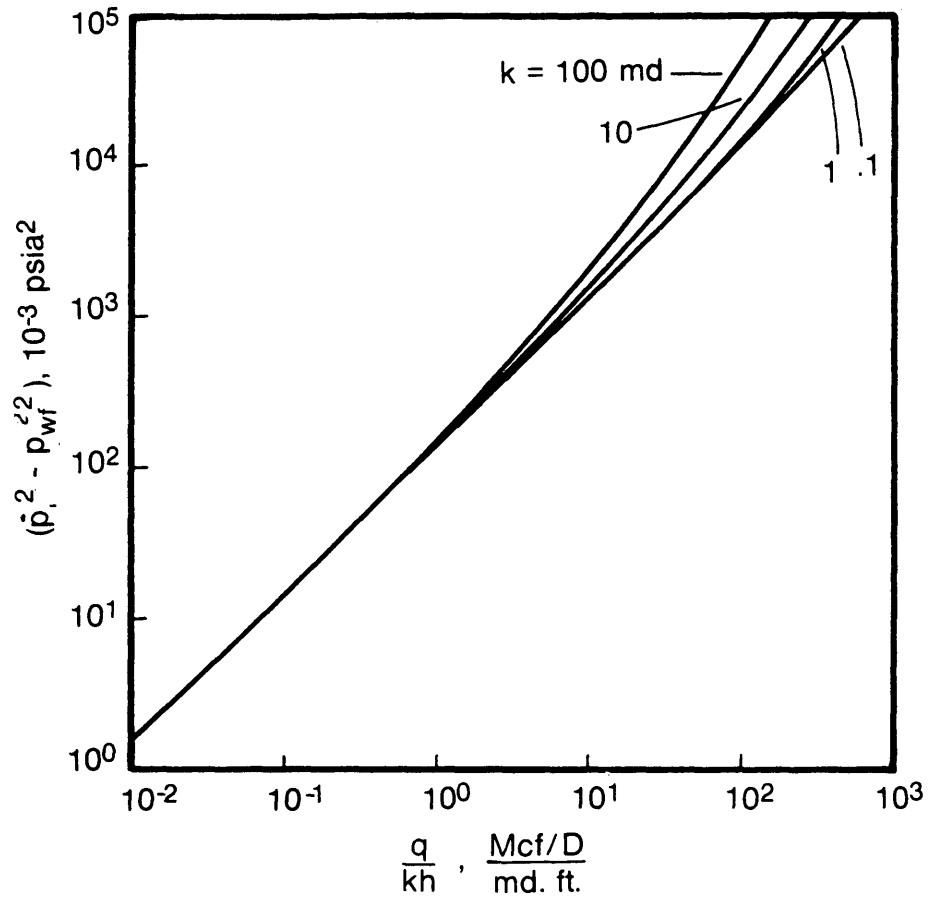


Figure 5. Normalize Backpressure Curve

Poettmann and Schilson described a procedure for calculating the variation of  $C_t$  with time from the modified Isochronal Test (20). For radial flow, they showed that the following relationship can be used:

$$C_t = \frac{C_1 \ln \left( \frac{\alpha}{a} t^{1/2} \right)^n}{\ln \left( \frac{\alpha}{a} t_1^{1/2} \right)^n} \quad (3)$$

where  $\alpha/a$  is defined as

$$\frac{\alpha}{a} = \frac{t_2 \frac{C_2^{1/n}}{2(C_1^{1/n} - C_2^{1/n})}}{t_1 \frac{C_1^{1/n}}{2(C_1^{1/n} - C_2^{1/n})}} \quad (4)$$

and  $C_1$  is the performance coefficient corresponding to a multipoint flow test with the flow duration equal to  $t_1$ ,  $C_t$  is the calculated performance coefficient corresponding to the flow duration equal to  $t$ .

Roger and Pascal investigated the effect of various drainage shapes on stabilized performance (21). Hadinoto and Tariq in separate work investigated the effect of infinite conductivity vertical fractures on stabilized

deliverability (24,25). In Hadinoto's work stabilized deliverability determined using conventional techniques will lead to erroneous values of predicted Absolute Open Flow (AOF) (23,24).

Tariq proposed the following relationship to be used until the end of linear flow:

$$C_t = C_l \frac{\sqrt{t_1^n}}{\sqrt{t^n}} \quad (5)$$

where  $t$  is the time to the end of linear flow (25). A radial flow assumption (Poettmann and Schilson) is then used to predict the stabilized value.

For finite conductivity fractures the method presented by Tariq will result in error. A finite conductivity vertically fractured well can exhibit linear, transitional, and radial flow (28,29,30,31,32,33,34,35,36). Application of only one flow type will lead to error in the prediction of stabilized deliverability.

In deeper wells (or where wellbore compressibility is large) wellbore storage (WBS) can influence early time data of a backpressure test (37,38). Backpressure tests affected by WBS will generally overestimate the AOF. Where WBS is large, test duration should extend beyond the influence of WBS.

## BACKPRESSURE TEST VALIDITY

### Flow-After-Flow-Test

For a properly conducted test under Darcy flow conditions a plot of  $\log (\bar{p}_R^2 - p_{wf}^2)$  versus  $\log q_{sc}$  will yield a slope of unity. Any deviation of the slope from unity is a result of non-Darcy flow. For this analysis it is assumed that non-Darcy flow provides a constant additional pressure drop over a limited flow rate range and its effect would only change the absolute slope. The validity of the flow-after-flow and isochronal tests can be evaluated by comparing a slope determined by rigorous application of the principle of superposition to the expected slope of unity for Darcy flow. Appendix A outlines the superposition analysis for flow-after-flow, isochronal, and modified isochronal tests.

A stabilized flow-after-flow test is one which reaches Pseudosteady-state during each flow period. Pseudosteady-state occurs when  $t = 1/4 t_D$  (38). Further, Pseudosteady-state commences when the pressure transient has reached the system boundary. At that time, pressure behavior becomes a function of reservoir depletion. In dimensionless form, the difference in pressure squared is equal to the flow rate times a constant (Appendix A). Since each

flow period reaches Pseudosteady-state, pressure drops no longer become a function of the log of time, and superposition of previous flow periods is not necessary. A plot of  $\log (\bar{p}_R^2 - p_{wf}^2)$  versus  $\log q_{sc}$  will yield a slope of one for Darcy flow.

The stabilized flow-after-flow test will provide the desired stabilized deliverability; however, it is limited to reservoirs having large permeability, which stabilize in a practical time frame. Stabilized flow-after-flow tests are seldom achieved.

An unstabilized flow-after-flow test does not achieve pseudosteady-state flow. Superposition is required to properly account for the continued influence of previous flow periods (Appendix A). The maximum dimensionless error, defined as deviation from the expected unit slope of the backpressure performance plot, for an unstabilized flow-after-flow is given by:

$$\Delta M_{BP} = \frac{\frac{q_{sc1}}{q_{sc4}} \ln \left(\frac{4}{3}\right) + \frac{q_{sc2}}{q_{sc4}} \ln \left(\frac{3}{2}\right) + \frac{q_{sc3}}{q_{sc4}} \ln (2)}{(\ln t_D + .8097 + s)} \quad (6)$$

As  $\Delta M_{BP} \rightarrow 0$ , the performance plot approaches the correct slope (in the case of Darcy flow, a slope of one).

Equation (6) illustrates the error sensitivity arising from the continued influence of previous flow periods in an unstabilized flow-after-flow test. Error can be minimized by reducing the flow rate ratio  $\frac{q_{sc1}}{q_{sc4}}$ ,  $\frac{q_{sc2}}{q_{sc4}}$ , and  $\frac{q_{sc3}}{q_{sc4}}$ , and by increasing  $t_D$ . For  $t_D$  greater than  $10^6$  the error is insignificant. Equation (6) is in dimensionless form so it applies to pressure, pressure squared and pseudo-pressure (or real gas potential) methods of analysis (39,40). It should be noted that equation (6) is not an absolute error in the slope of the performance plot, but is a deviation. Slope deviation goes to zero as equation (6) goes to zero.

A flow-after-flow test would not be the test of choice unless stabilized flow can reasonably be achieved. Error sensitivity has been calculated by applying rigorous superposition using base case parameters given in Table 1. Superposition of multiple flow periods was used to determine the pressure for each flow period. The rate and pressure results were then analyzed using the Rawlins and Schellhardt technique. Figure 6 shows error in flow exponent "n". An unstabilized flow-after-flow test will underestimate "n". Table 2 shows how error can be reduced by increasing the flow time (approach a stabilized test), and

by decreasing the flow rate ratios using a normal sequence. In unstabilized flow-after-flow, these errors result in an erroneous  $C_S$ , making any stabilized deliverability prediction questionable.

### Isochronal Test

An isochronal test requires that static reservoir pressure be reached during the shut-in period. The isochronal test is based on the principle that the drainage radius established during a flow period is a function only of dimensionless time and is independent of flow rate (41). For equal flow times the same drainage radius is established for the different flow rates. Since the shut-in periods reach static pressure, no superposition of shut-ins are necessary. Superposition of the flow periods results in the squared pressure difference equal to the flow rate multiplied by a constant, and will yield unit slope (Appendix A).

Table 1

**Base Case Parameters**

---

k	10 md
h	10 ft
$\phi$	10%
$r_e$	1000 ft
$r_w$	.25 ft
s	0.0
$T_{res}$	150° F
$T_B$	60° F
$p_i$	3000 psia
$p_B$	14.7 psia
$\bar{z}$	0.95
$\bar{\mu}$	.02 cp
$\bar{c}$	0.0003 psi <sup>-1</sup>
$q_{sc1}$	1 MMSCF/D
$q_{sc2}$	2 MMSCF/D
$q_{sc3}$	3 MMSCF/D
$q_{sc4}$	4 MMSCF/D
$t_f$	4 hrs

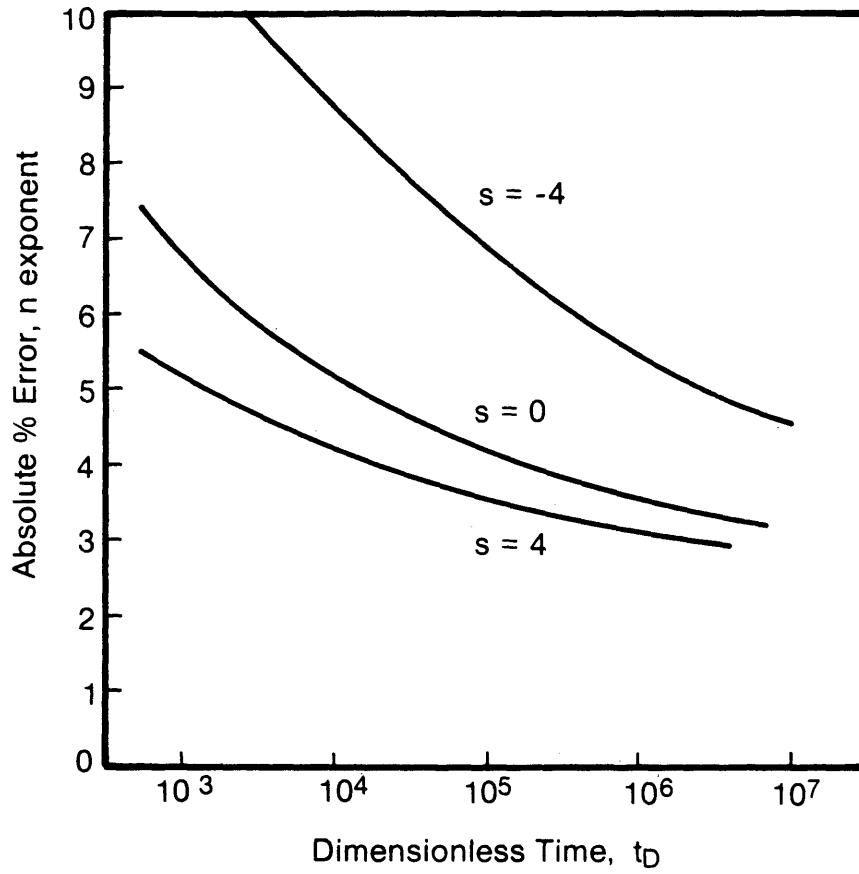


Figure 6. Absolute Error in "n" - Flow-After-Flow Test

**Table 2**  
**Sensitivity of Error in "n" to Flow Rate Ratio**  
**and Sequence**  
**Flow-After-Flow Test**

$q_{sc1}$	$q_{sc2}$	$q_{sc3}$	$q_{sc4}$	n	% error
1.00	1.25	1.50	1.75	.8609	13.91
1.00	1.50	2.00	2.50	.9202	7.98
1.00	2.00	3.00	4.00	.9526	4.74
1.00	4.00	8.00	16.00	.9846	1.54
1.75	1.50	1.25	1.00	1.4026	-40.26
2.50	2.00	1.50	1.00	1.2855	-28.55
4.00	3.00	2.00	1.00	1.2597	-25.97
16.00	8.00	4.00	1.00	1.3246	-32.46

The isochronal test provides a valid, but transient deliverability. An extended flow test or a computational method is necessary for calculating the stabilized performance coefficient.

### Modified Isochronal Test

The modified isochronal test does not reach a static pressure during the shut-in periods. Normally, the final shut-in pressure reached is used in place of the static reservoir pressure in the backpressure expression. Flow and shut-in periods must use superposition to properly account for their continued influence with time (Appendix A). The maximum dimensionless error for a modified isochronal test is given by:

$$\begin{aligned} \Delta M_{BP} = & \left( \frac{q_{sc1}}{q_{sc4}} \ln \frac{8(t_f/t_s)^2 + 18(t_f/t_s) + 9}{9(t_f/t_s)^2 + 18(t_f/t_s) + 9} \right. \\ & + \frac{q_{sc2}}{q_{sc4}} \ln \frac{3(t_f/t_s)^2 + 8(t_f/t_s) + 9}{4(t_f/t_s)^2 + 8(t_f/t_s) + 9} \\ & \left. + \frac{q_{sc3}}{q_{sc4}} \ln \frac{2(t_f/t_s) + 1}{(t_f/t_s)^2 + 2(t_f/t_s) + 1} \right) / (\ln t_D + .8097 + s) \end{aligned} \quad (7)$$

For a modified isochronal test where shut-in and flow times are equal, the maximum error is given by:

$$\Delta M_{BP} = \frac{\frac{q_{sc1}}{q_{sc4}} \ln \left( \frac{35}{36} \right) + \frac{q_{sc2}}{q_{sc4}} \ln \left( \frac{15}{16} \right) + \frac{q_{sc3}}{q_{sc4}} \ln \left( \frac{3}{4} \right)}{(\ln t_D + .8097 + s)} \quad (8)$$

Once again,  $\Delta M_{BP}$  is not an absolute error. As  $\Delta M_{BP} \rightarrow 0$  the performance plot approaches the correct slope. Equations (7) and (8) illustrate the error sensitivity resulting from the continued influence of previous flow and shut-in periods in a modified isochronal test. Equations (7) and (8) apply to pressure, pressure squared or pseudo-pressure methods of analysis. In a fashion similar to that for a flow-after-flow test, the error can be reduced by decreasing the flow rate ratio  $\left( \frac{q_{sc1}}{q_{sc4}}, \frac{q_{sc2}}{q_{sc4}}, \text{ and } \frac{q_{sc3}}{q_{sc4}} \right)$  using a normal flow sequence, and by increasing  $t_D$ . A  $t_D$  greater than  $10^5$  results in insignificant error. Equation (7) shows another means of reducing the superposition error by conducting a modified isochronal test with flow periods of shorter duration than the shut-in periods.

Rigorous superposition of flow and shut-in periods was used to determine the pressure for each flow period. The rate and pressure data were analyzed using the Rawlins and Schellhardt technique. The absolute errors determined are based on the parameters given in Table 1.

Such an analysis shows that a modified isochronal test will overestimate "n". However, for equal flow durations, the modified isochronal test will result in 1/3 the error in "n" compared to an unstabilized flow-after-flow test (Figs. 7-8).

It is not a requirement that flow time be equal to shut-in time. Considerable reduction in "n" error can be realized for flow time to shut-in time ratio less than one (Fig. 9). A modified isochronal test with equal flow and shut-in periods will result in twice the error in "n" when compared to a test with a flow time to shut-in time ratio of 0.5. Error in "n" can also be reduced by decreasing flow rate ratios in a normal sequence (Table 3).

The flow-after-flow and isochronal tests are valid. If conditions permit, these tests are preferred. An unstabilized flow-after-flow test is not desirable. If stabilized flow-after-flow and isochronal tests are not practical as a result of time or economic constraints, a modified isochronal test should be considered. The modified isochronal test has insignificant error for dimensionless time greater than  $10^5$ . It has been demonstrated that error can be reduced further if a normal flow sequence is used, and if the flow rate change is maximized (42). It has also been demonstrated that error can be reduced even further if

flow time is less than shut-in time as opposed to the generally accepted equal flow and shut-in time.

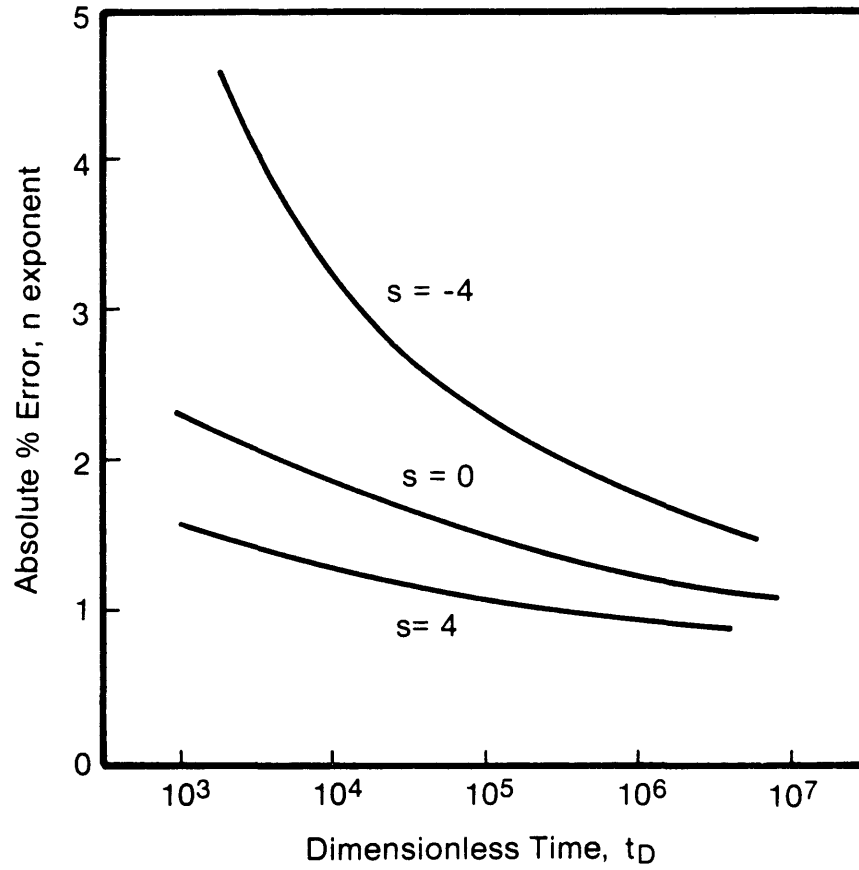


Figure 7. Absolute Error in "n" - Modified Isochronal Test

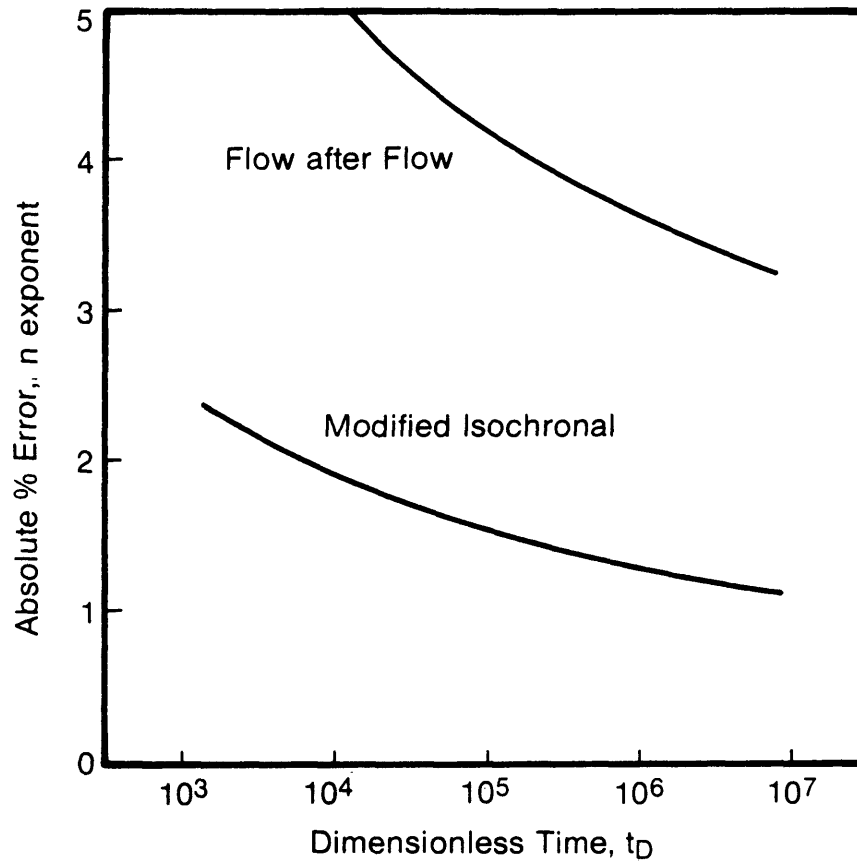
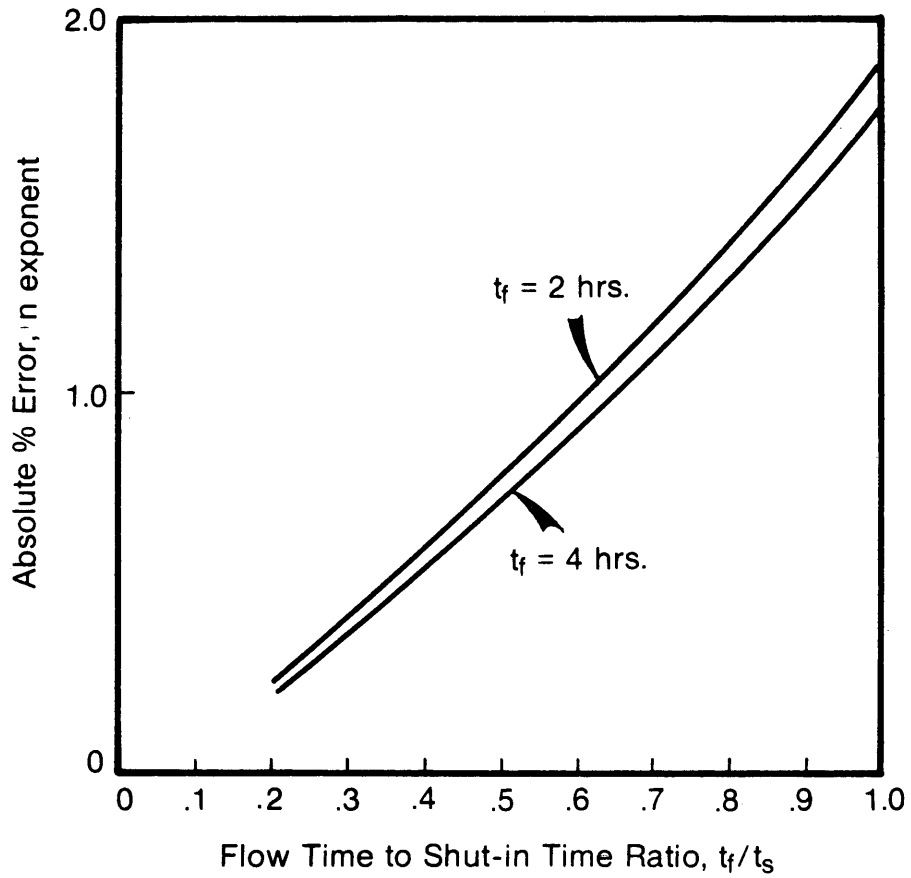


Figure 8. Comparison of Error Between an Unstabilized Flow-After-Flow Test and Modified Isochronal Test



**Figure 9. Absolute Error in "n" for Flow Time To Shut-In Time Ratio Less Than One - Modified Isochronal Test**

**Table 3**  
**Sensitivity of Error in "n" to Flow Rate Ratio**  
**and Sequence**  
**Modified Isochronal Test**

$q_{sc1}$	$q_{sc2}$	$q_{sc3}$	$q_{sc4}$	n	% error
1.00	1.25	1.50	1.75	1.0524	-5.25
1.00	1.75	2.00	2.50	1.0288	-2.88
1.00	2.00	3.00	4.00	1.0173	-1.73
1.00	4.00	8.00	12.00	1.0076	-0.76
1.00	8.00	16.00	24.00	1.0056	-0.56
1.75	1.50	1.25	1.00	.9279	7.21
2.50	2.00	1.50	1.00	.9441	5.59
4.00	3.00	2.00	1.00	.9471	5.29
12.00	8.00	4.00	1.00	.9268	7.32
24.00	16.00	8.00	1.00	.8733	12.67

The absolute errors have been presented to illustrate the sensitive parameters so as to aid in the design of a backpressure test. Figures 6, 7 and 9 should not be used for correcting backpressure tests.

The errors discussed are those that affect the flow exponent (or slope of the backpressure curve). No attempt has been made to determine the stabilized deliverability from the transient deliverability. However, if confidence in the slope of the backpressure curve is achieved, then an extended flow (stabilized flow) can be used. Then the stabilized deliverability is plotted parallel to the transient deliverability through the extended flow point.

In addition, the minimum flow time should be selected to allow wellbore storage effects to disappear, and the minimum flow rate should be capable of unloading the wellbore of any accumulated liquids.

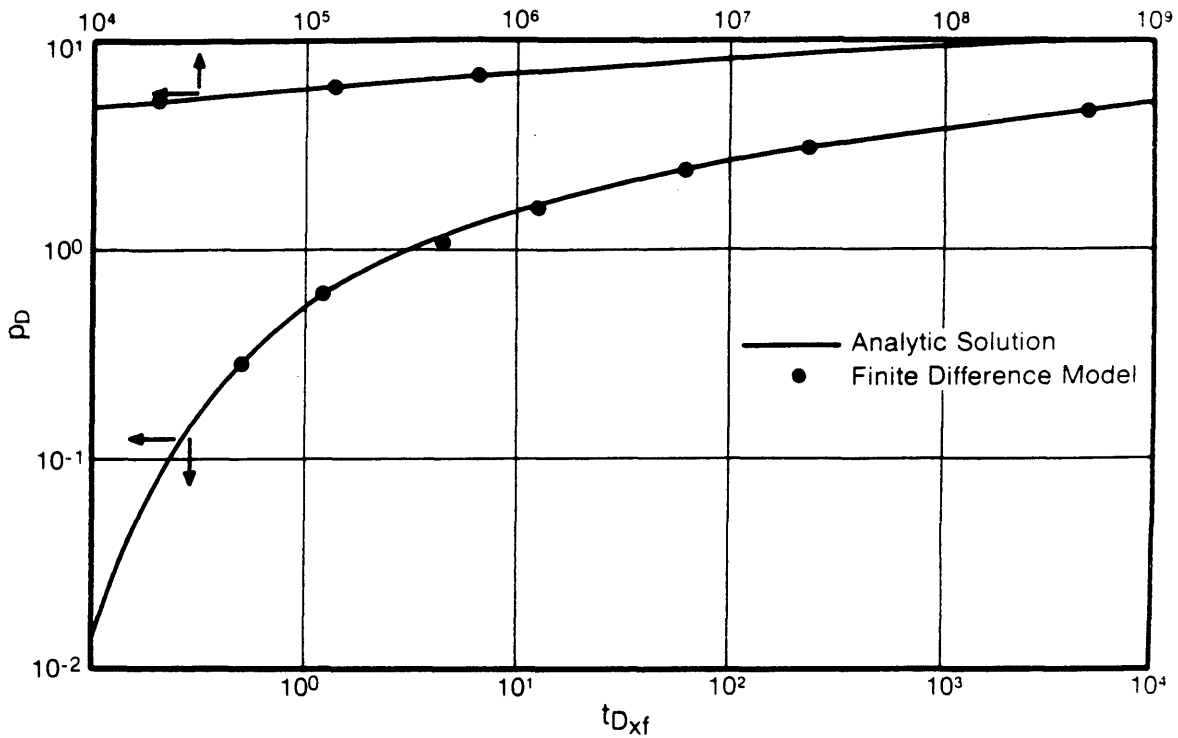
It is important to note that the superposition error also applies in a qualitative manner to the Forchheimer expression.

### DELIVERABILITY OF VERTICALLY FRACTURED WELLS

The isochronal test combined with techniques to obtain stabilized back-pressure behavior has become a standard procedure for estimating the stabilized deliverability of a well. Interpretation of these tests has traditionally been based on solutions for radial flow; however, a serious problem exists in the case of a hydraulically fractured gas well. Linear and transitional flow behavior in a hydraulically fractured well can potentially last hundreds of hours. Millheim and Cichowicz reported stabilized performance was not obtained for fractured gas wells in the San Juan Basin and the early pressure behavior deviated from radial flow (30).

The applicability of the radial flow assumption for a well with a finite conductivity vertical fracture has been examined. In this study isochronal tests were generated using a fully-implicit two-dimensional gas reservoir simulator. Fracture lengths of 10 to 2000 feet and dimensionless conductivities of 0.1 to 100 were investigated.

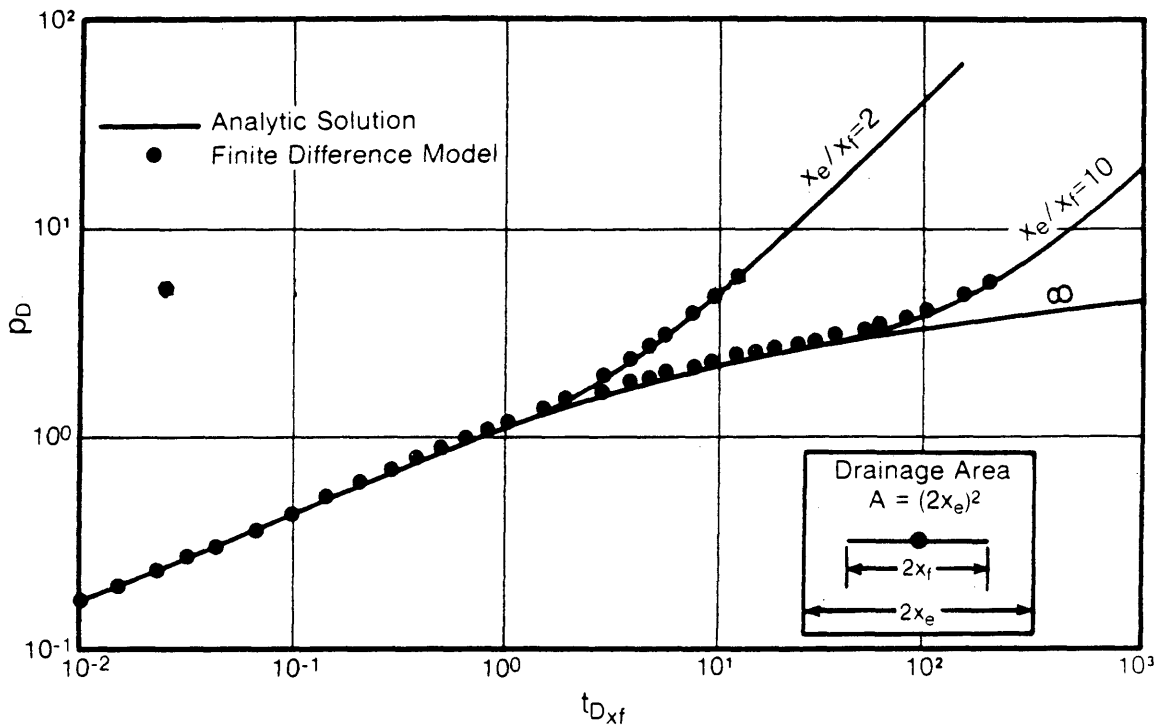
The validity of the simulator was demonstrated by comparing it to analytical solutions. Figure 10 compares the numerical simulator to the line source solution. Figure 11 compares the simulator to analytical solutions for infinite conductivity fractures in bounded systems. Figure 12



Line Source Solution  
(after H.R. Ramey, Jr.)

Figure 10. Comparison of Numerical Simulator to Line Source Solution

ARTHUR LAKES LIBRARY  
 COLORADO SCHOOL of MINES  
 GOLDEN, COLORADO 80401



(after Gringarten, Ramey and Rayhaven)

**Figure 11. Comparison of Numerical Simulator to Analytical Solution for Infinite Conductivity Vertical Fractures in Bounded Systems**

compares the simulator to an analytical solution for finite conductivity vertical fractures.

The numerical simulator was used to generate isochronal tests under Darcy flow. The simulated isochronal tests are shown in Figures 13 through 25. The simulation results provided values of  $n = 1$  for all cases. There was no apparent sensitivity of flow exponent to fracture conductivity or length. However, the performance coefficient depended on flow time and dimensionless fracture conductivity. This unique relationship is shown in Figure 26.

The performance coefficient, when Pseudosteady-state has not been reached, is a function of time, reservoir parameters, and flow geometry. If a non-applicable flow geometry is used to predict the stabilized performance coefficient, then considerable error in stabilized deliverability can result. Based on the simulation results, a radial flow projection, when  $C_t$  is in a linear or transitional flow, will considerably overestimate the stabilized well deliverability (Figure 27). Similarly, a linear flow projection will underestimate deliverability (Figure 28). Error in stabilized deliverability will still result if a linear flow extrapolation is used until the beginning of radial flow (Figure 29) and a radial flow extrapolation from that point forward (Figure 30).

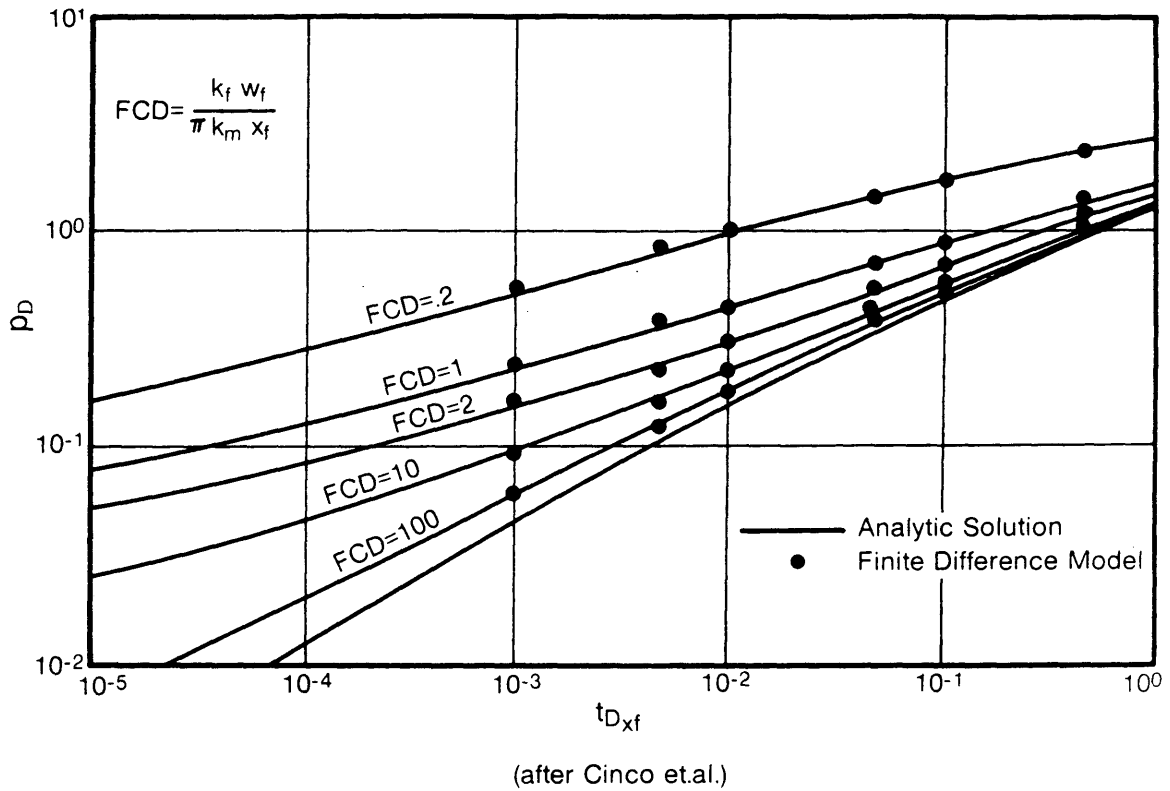


**Figure 12. Comparison of Numerical Simulator to Analytical Solution for Finite Conductivity Vertical Fractures**

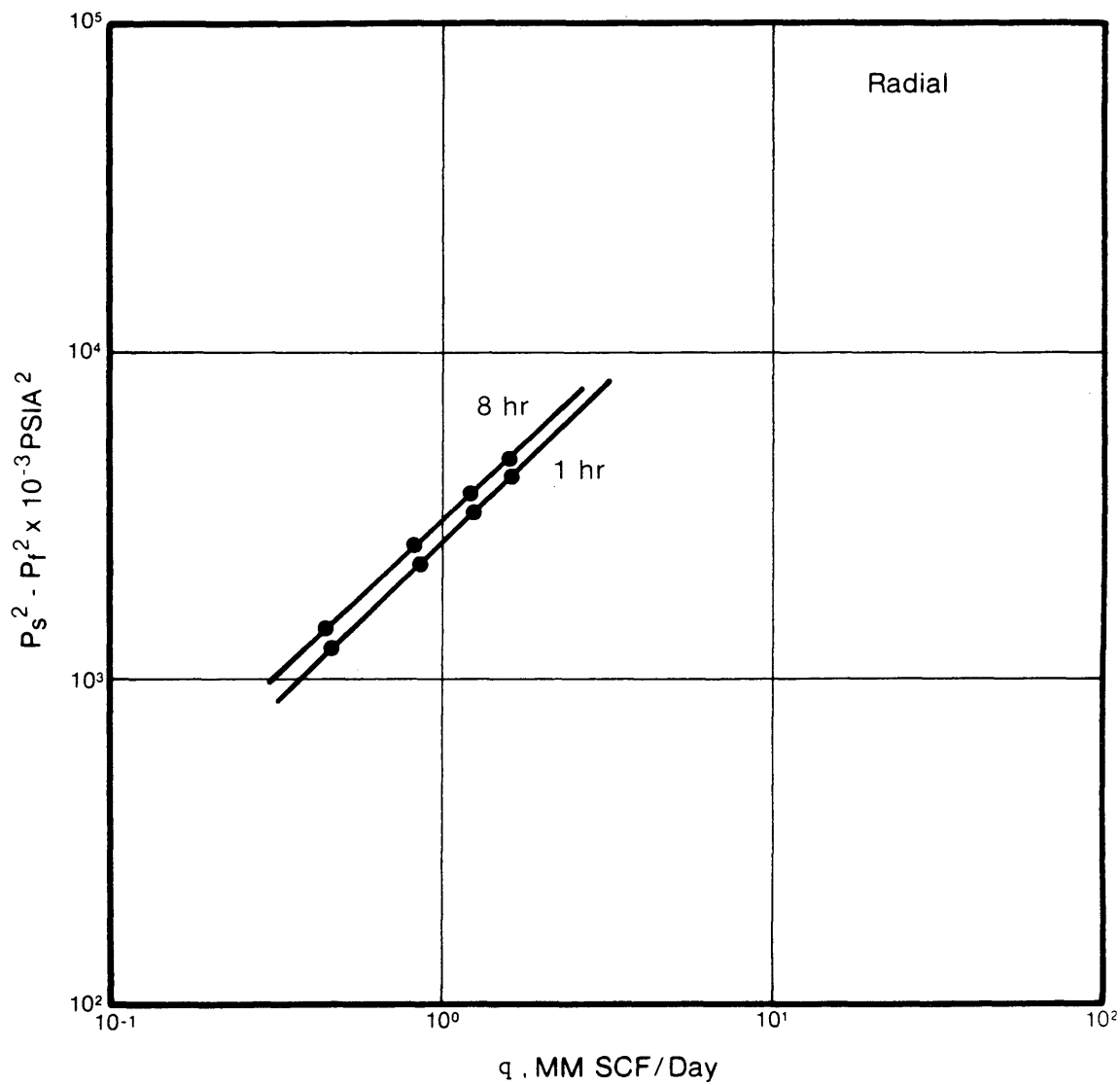


Figure 13. Simulated Isochronal Test, Radial Flow

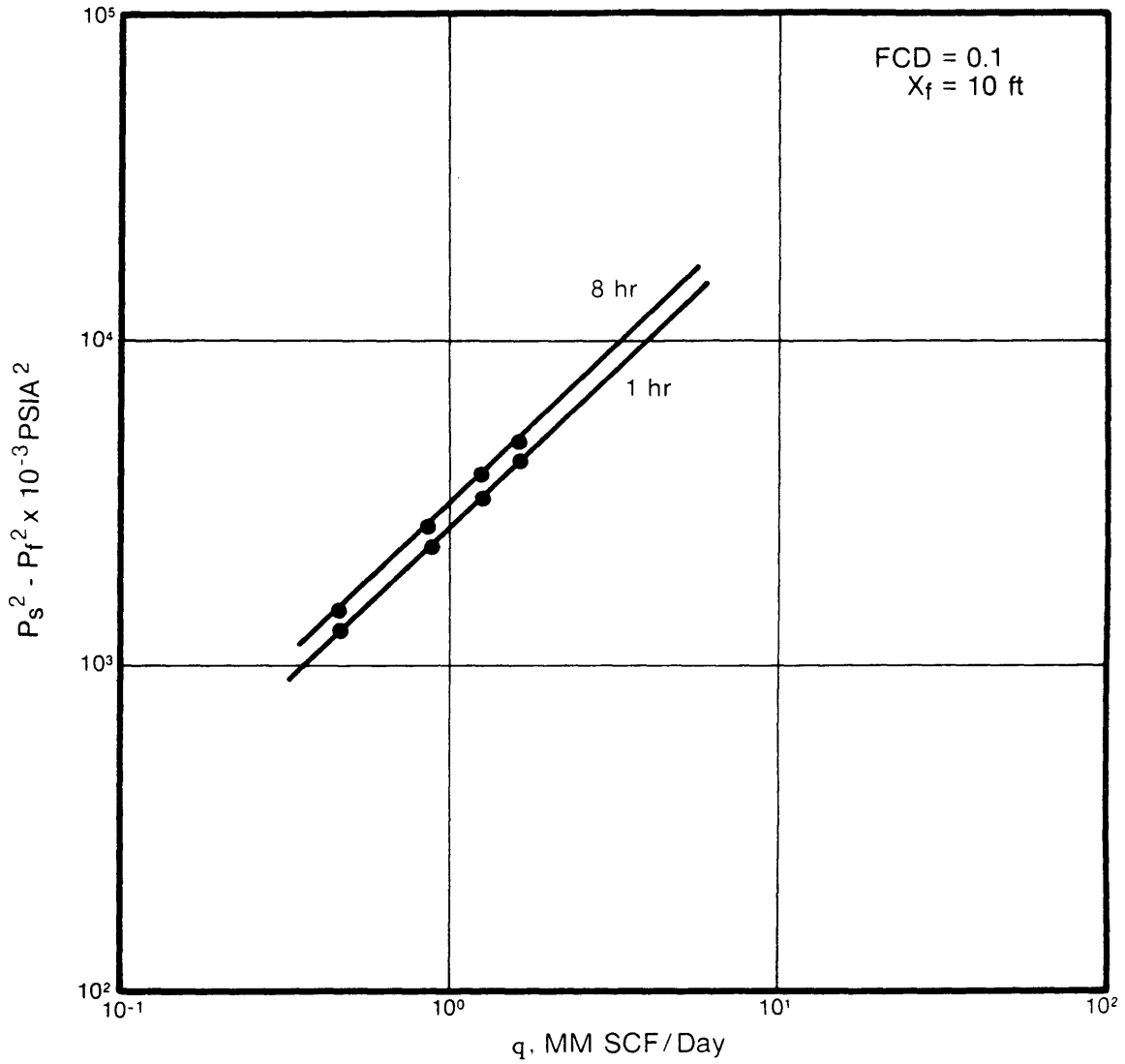


Figure 14. Simulated Isochronal Test, Finite Conductivity Vertical Fracture ( $F_{CD} = 0.1$   $X_f = 10 \text{ ft}$ )

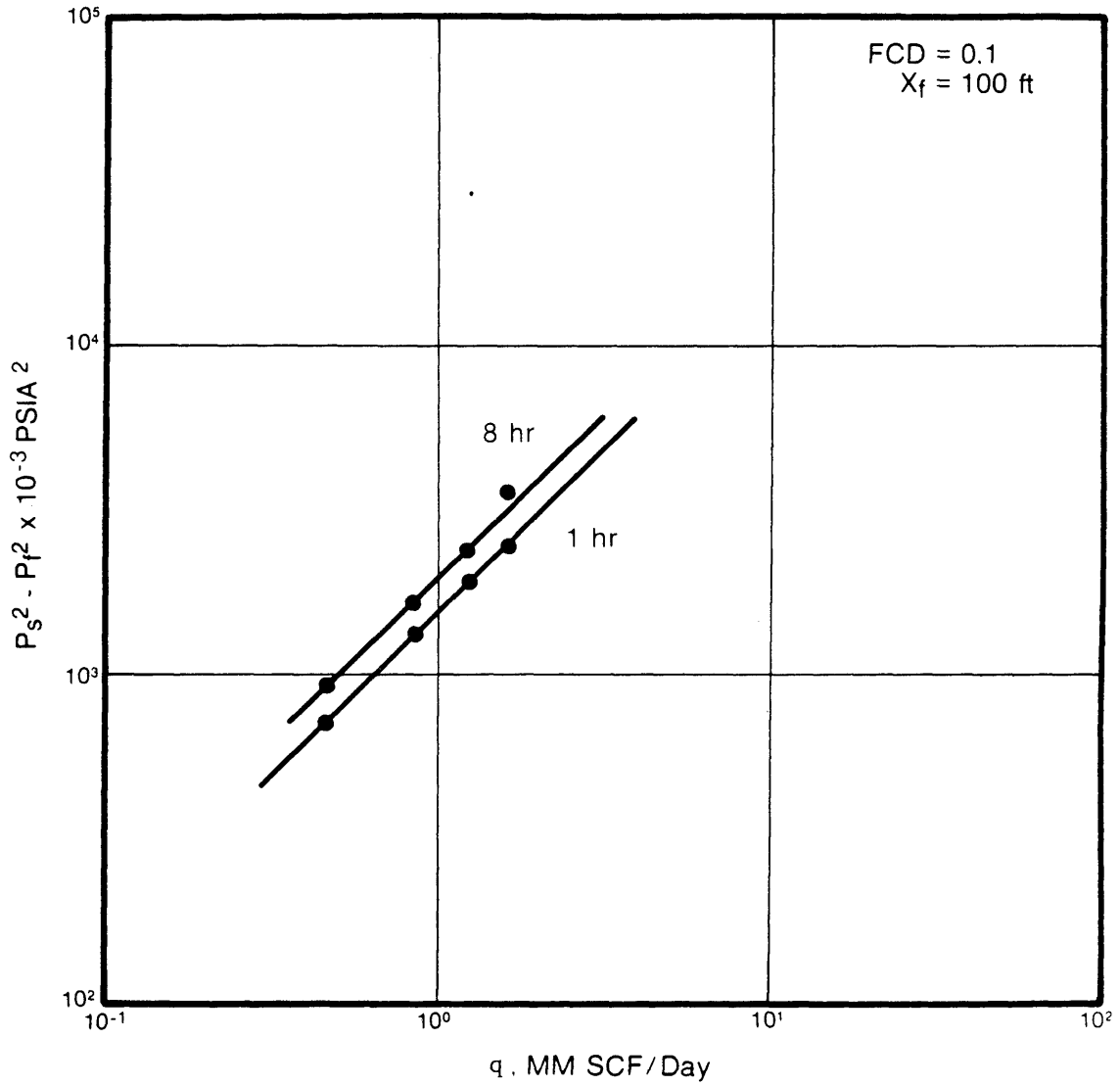


Figure 15. Simulated Isochronal Test, Finite Conductivity Vertical Fracture ( $F_{CD} = 0.1$   $X_f = 100$  ft)

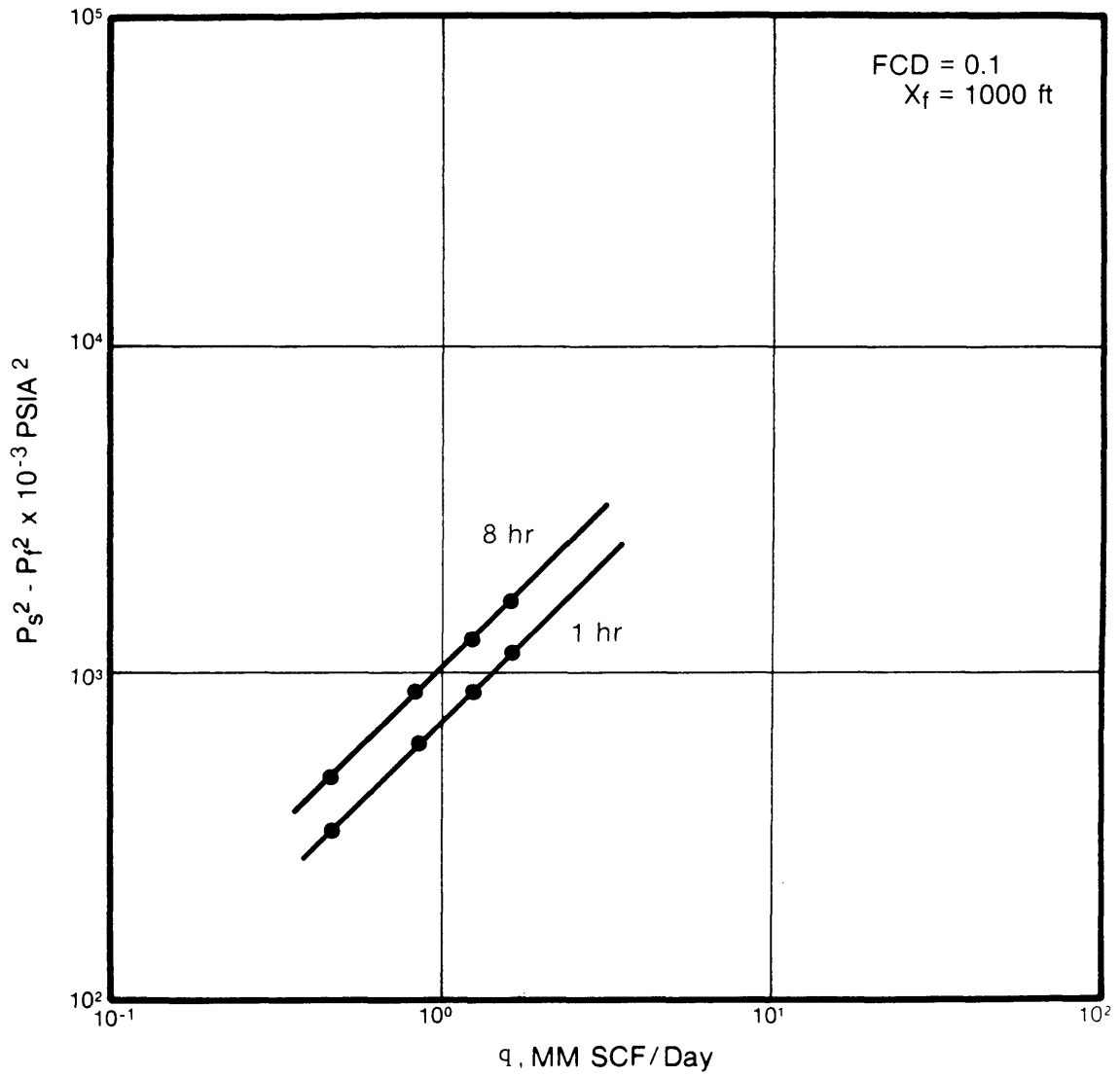


Figure 16. Simulated Isochronal Test, Finite Conductivity Vertical Fracture ( $FCD = 0.1$   $X_f = 1000 \text{ ft}$ )

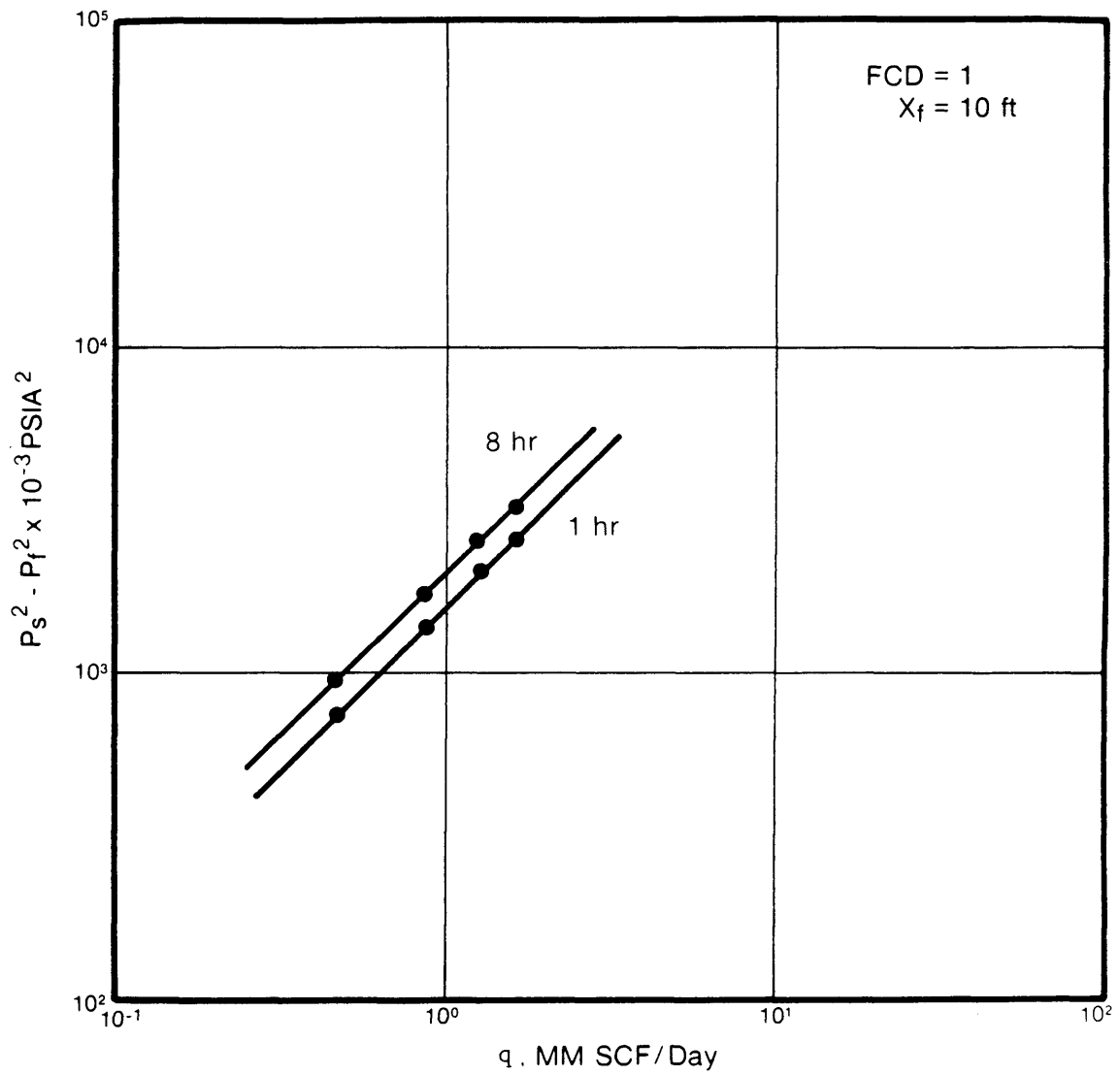


Figure 17. Simulated Isochronal Test, Finite Conductivity Vertical Fracture ( $FCD = 1.0$   $X_f = 10 \text{ ft}$ )

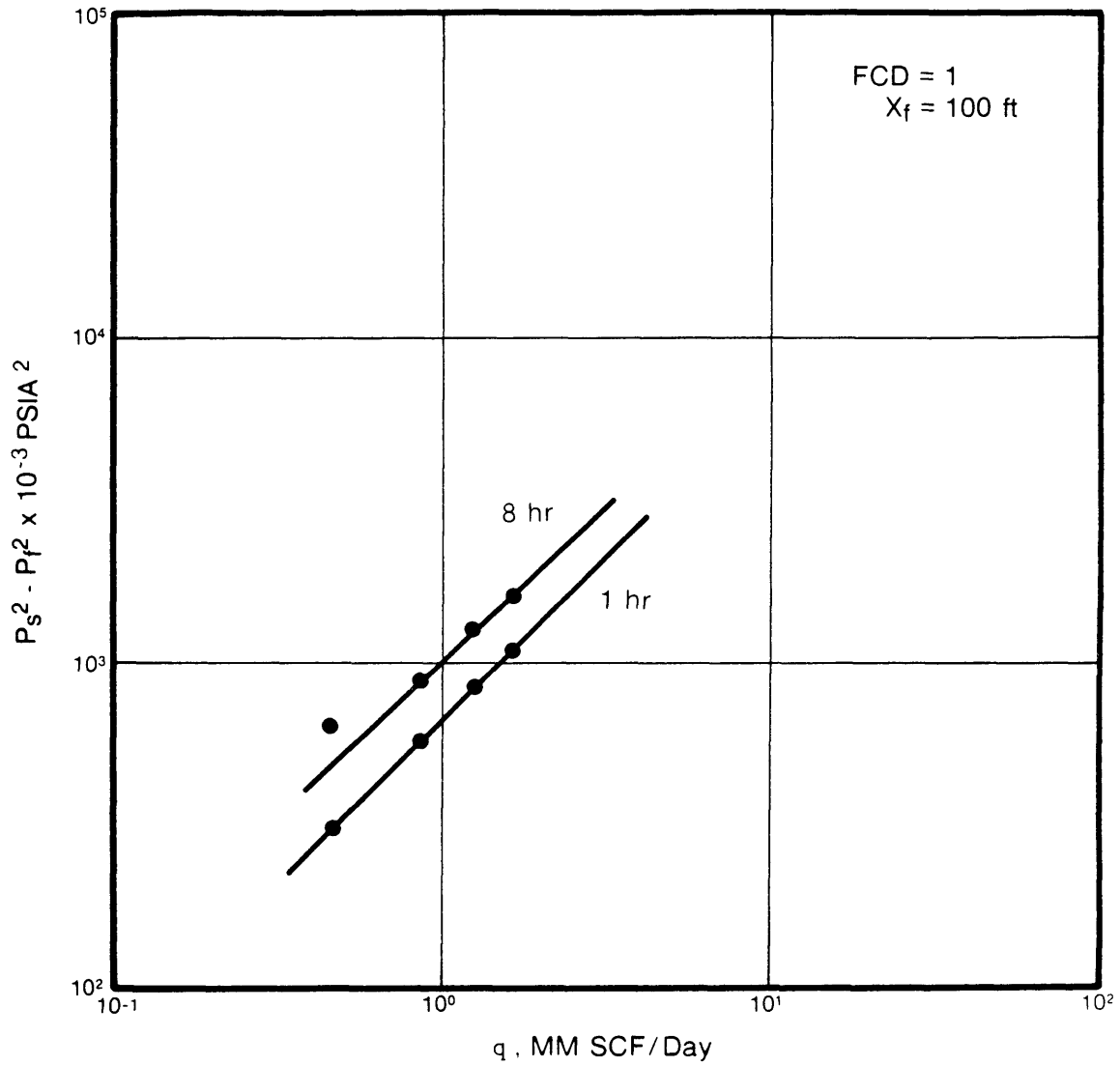


Figure 18. Simulated Isochronal Test, Finite Conductivity Vertical Fracture ( $FCD = 1.0$   $X_f = 100 \text{ ft}$ )

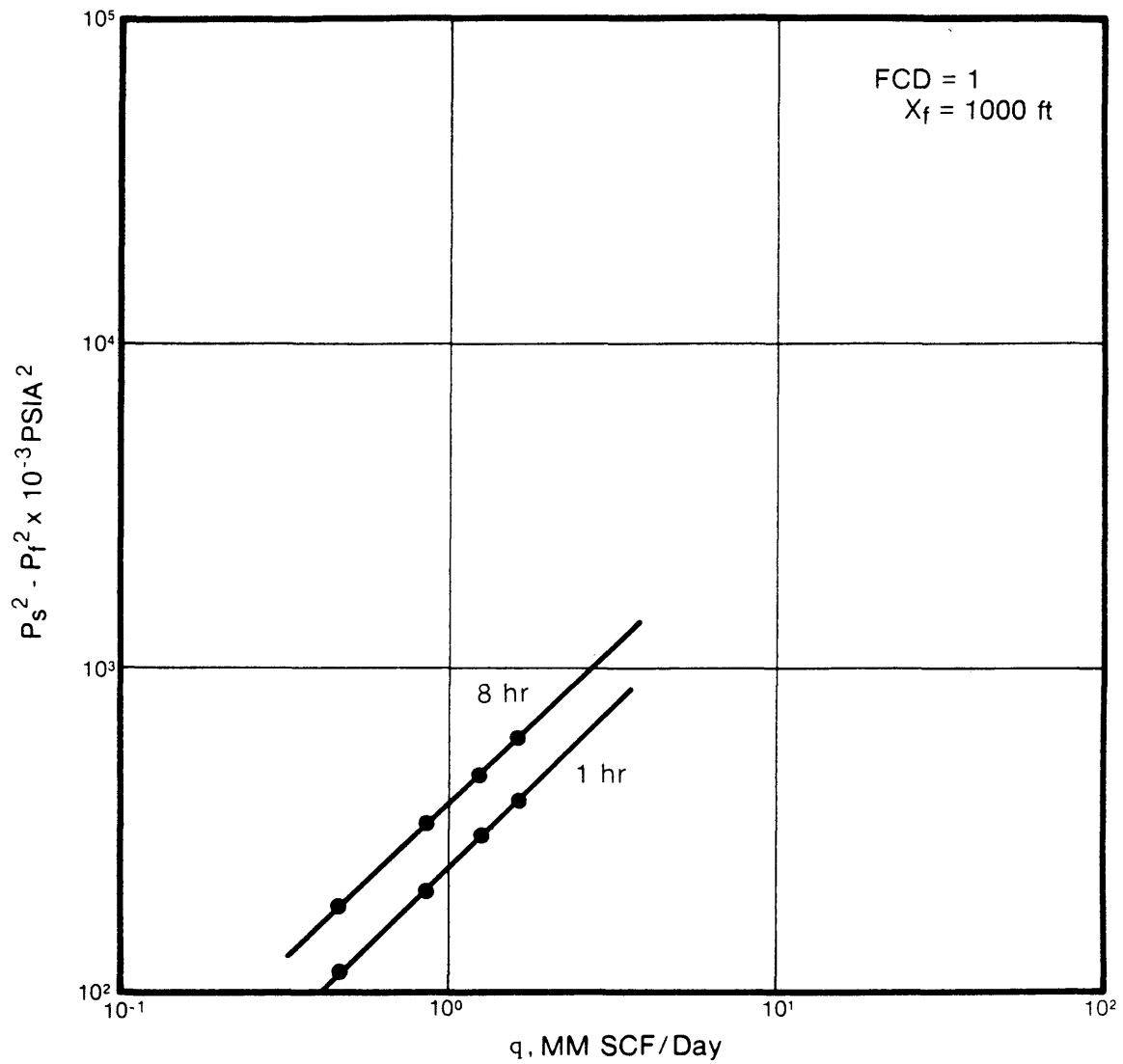


Figure 19. Simulated Isochronal Test Finite Conductivity Vertical Fracture ( $F_{CD} = 1.0$   $X_f = 1000 \text{ ft}$ )

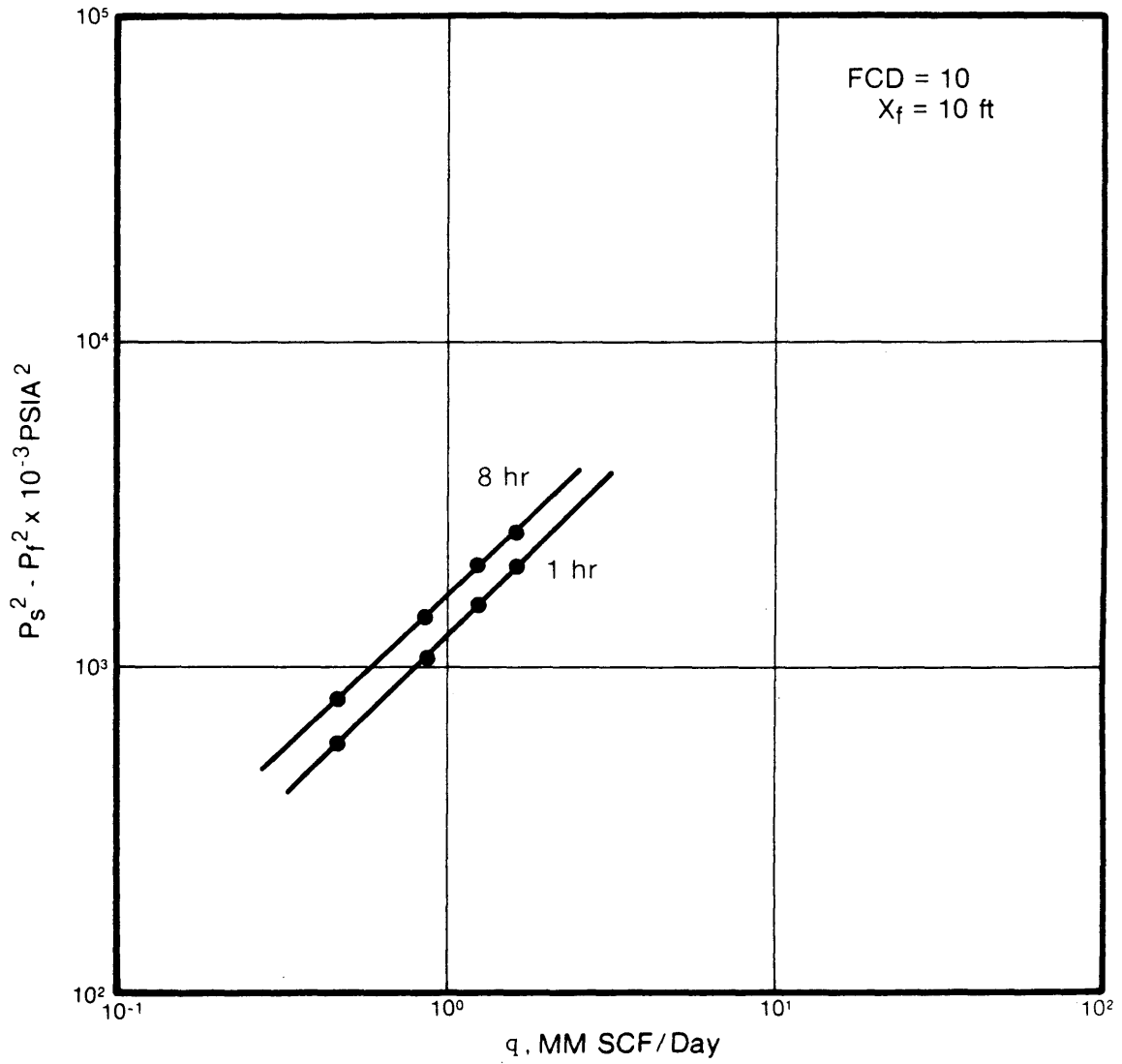


Figure 20. Simulated Isochronal Test Finite Conductivity Vertical Fracture ( $F_{CD} = 10$   $X_f = 10 \text{ ft}$ )

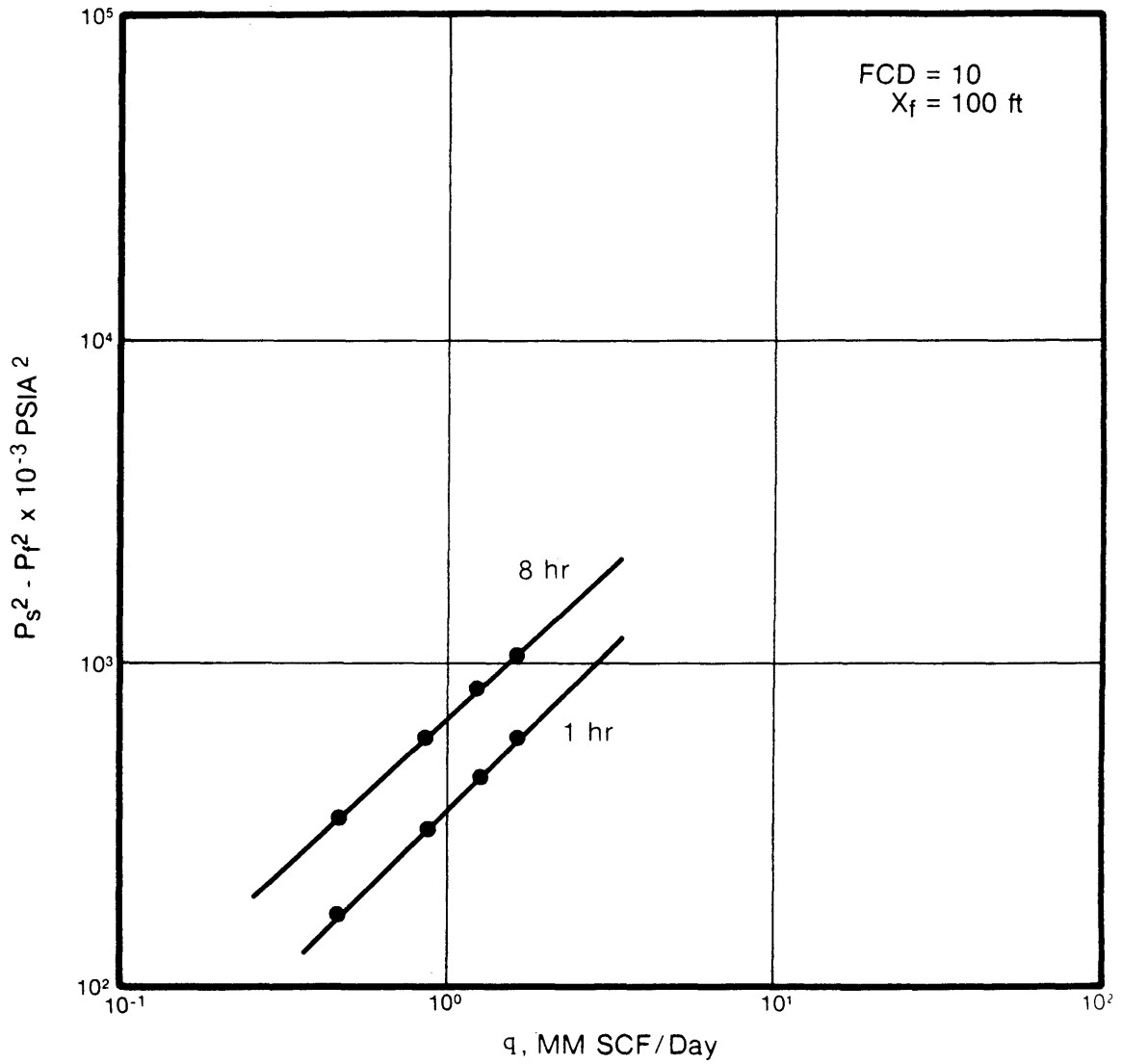


Figure 21. Simulated Isochronal Test Finite Conductivity Vertical Fracture (FCD = 10 X<sub>f</sub> = 100 ft)

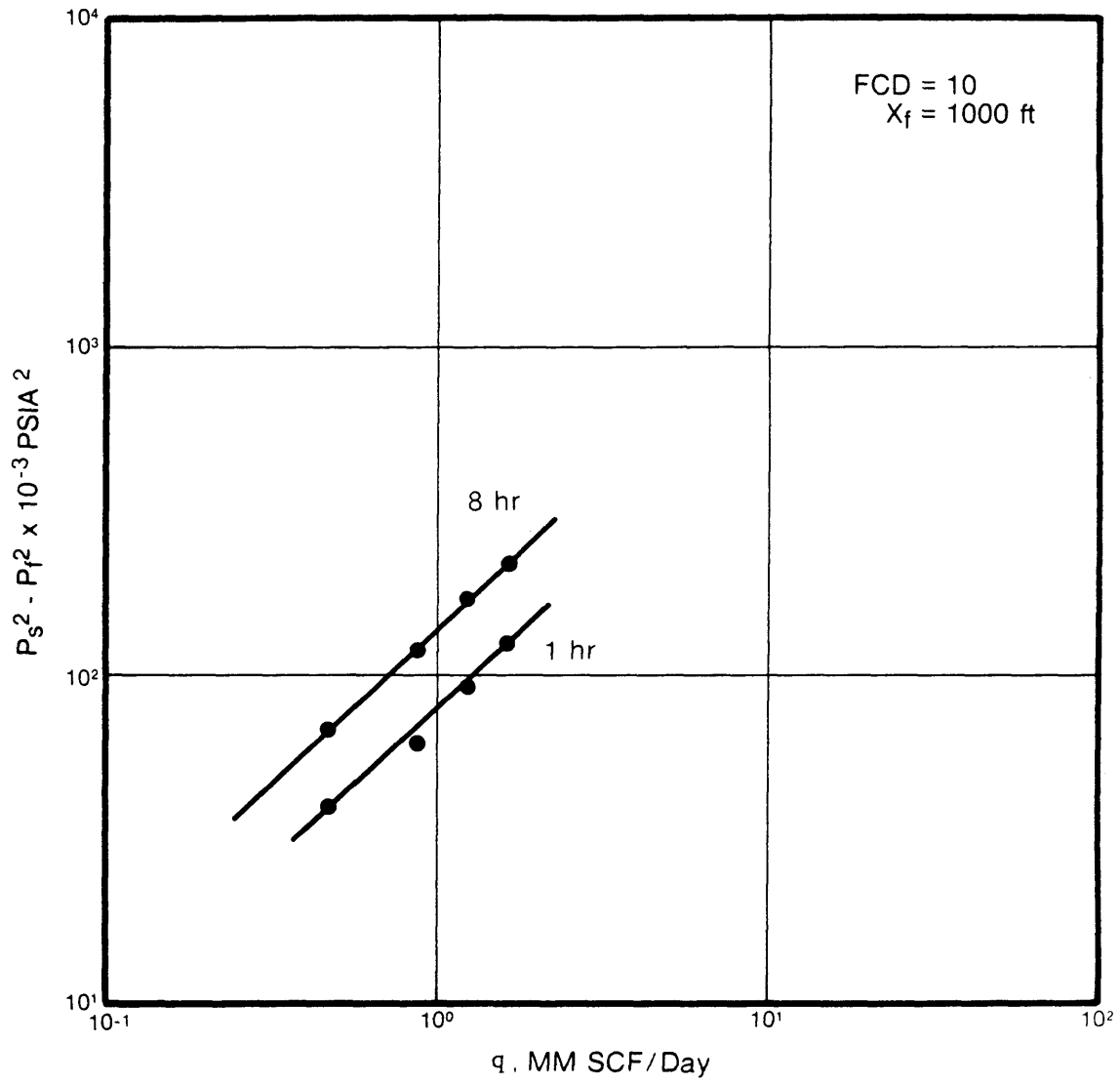


Figure 22. Simulated Isochronal Test Finite Conductivity Vertical Fracture ( $F_{CD} = 10$   $X_f = 1000 \text{ ft}$ )

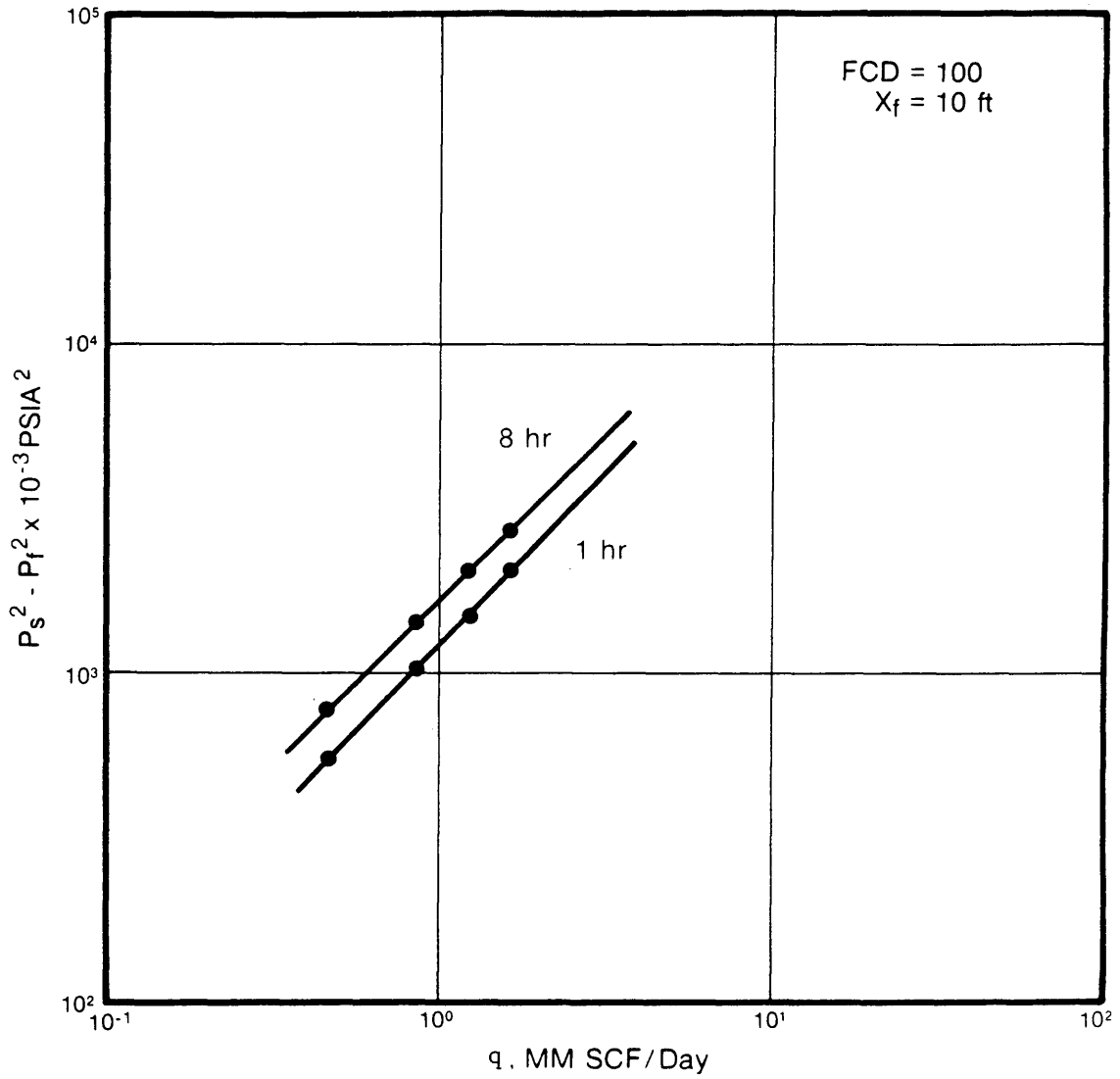


Figure 23. Simulated Isochronal Test Finite Conductivity Vertical Fracture ( $F_{CD} = 100$   $X_f = 10 \text{ ft}$ )

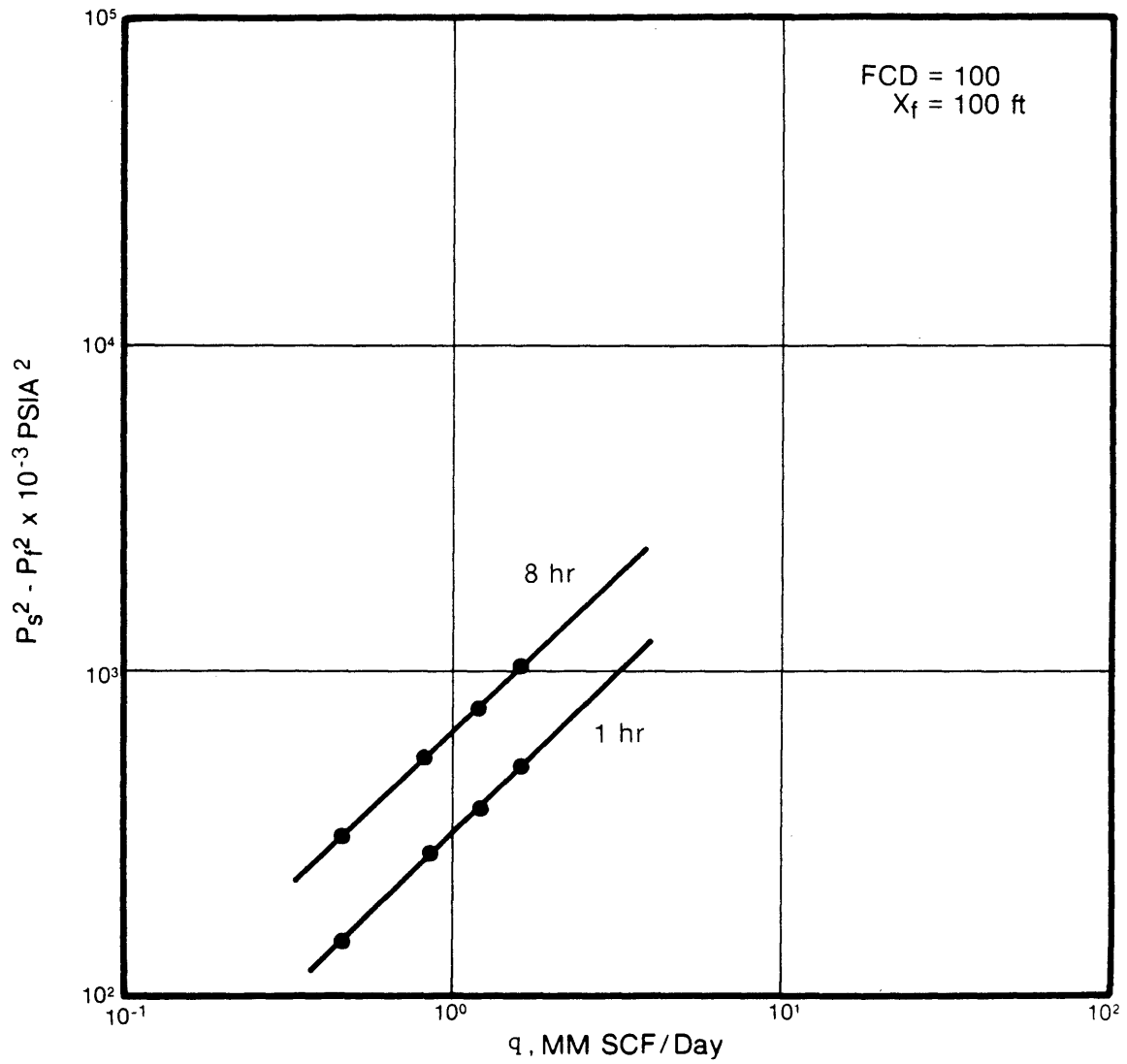


Figure 24. Simulated Isochronal Test Finite Conductivity Vertical Fracture ( $F_{CD} = 100$   $X_f = 100 \text{ ft}$ )

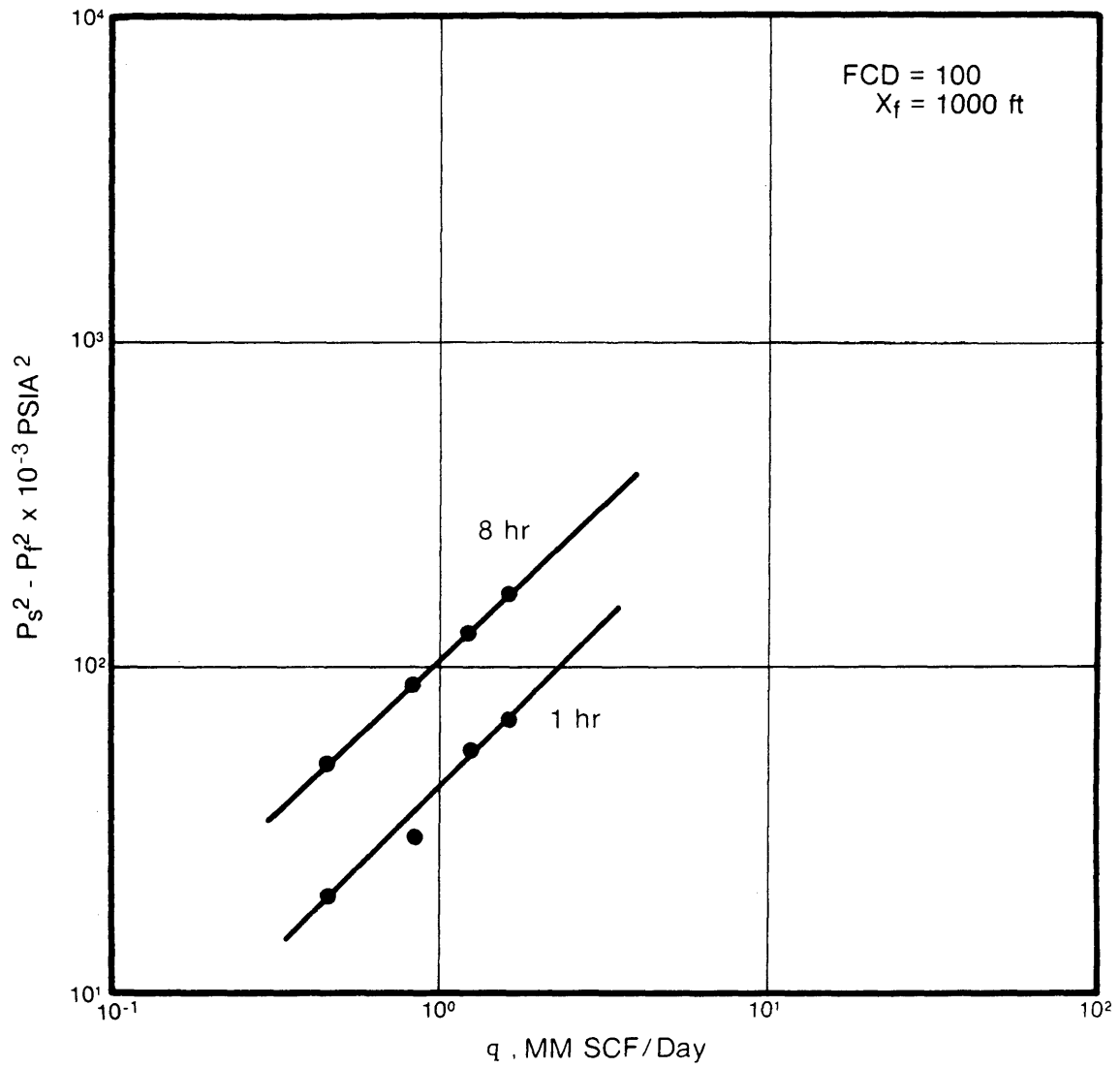


Figure 25. Simulated Isochronal Test Finite Conductivity Vertical Fracture ( $F_{CD} = 100$   $X_f = 1000 \text{ ft}$ )

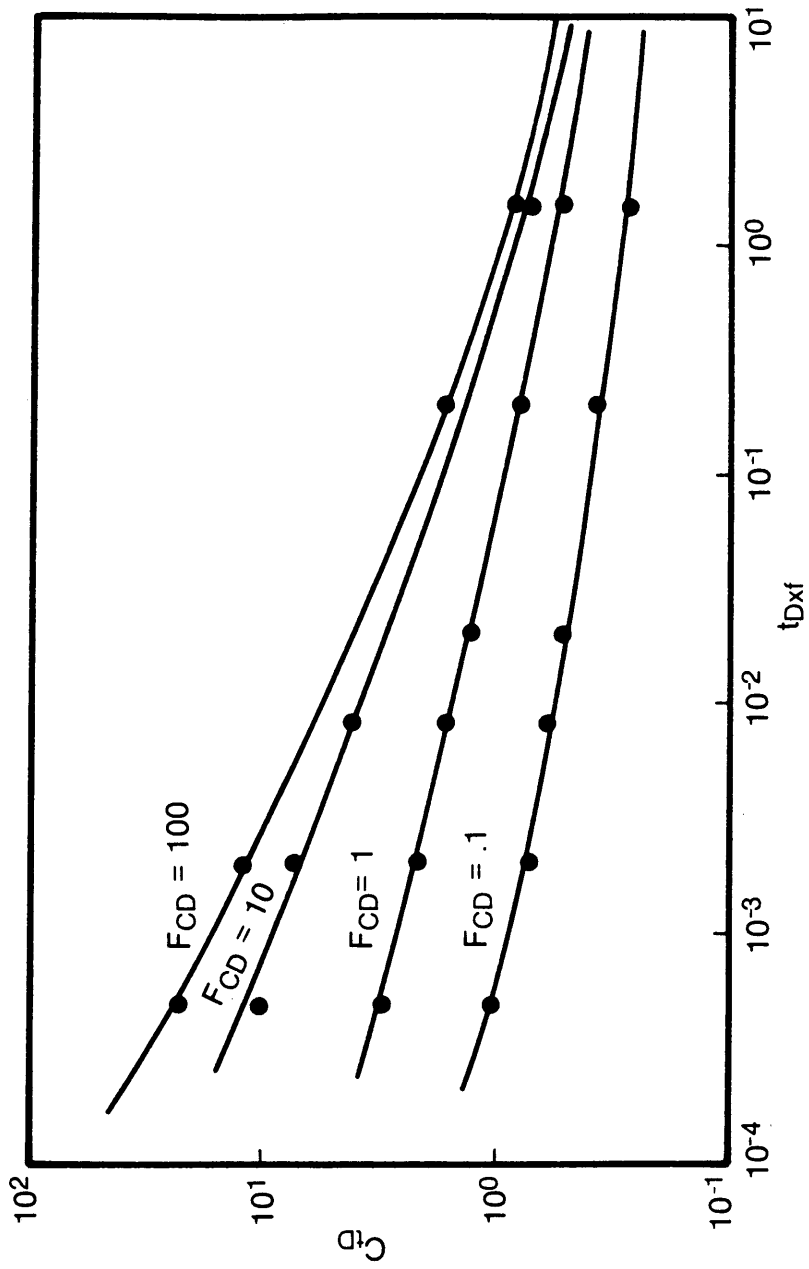


Figure 26. Dimensionless Performance Coefficient for a Finite Conductivity Vertically Fractured Gas Well

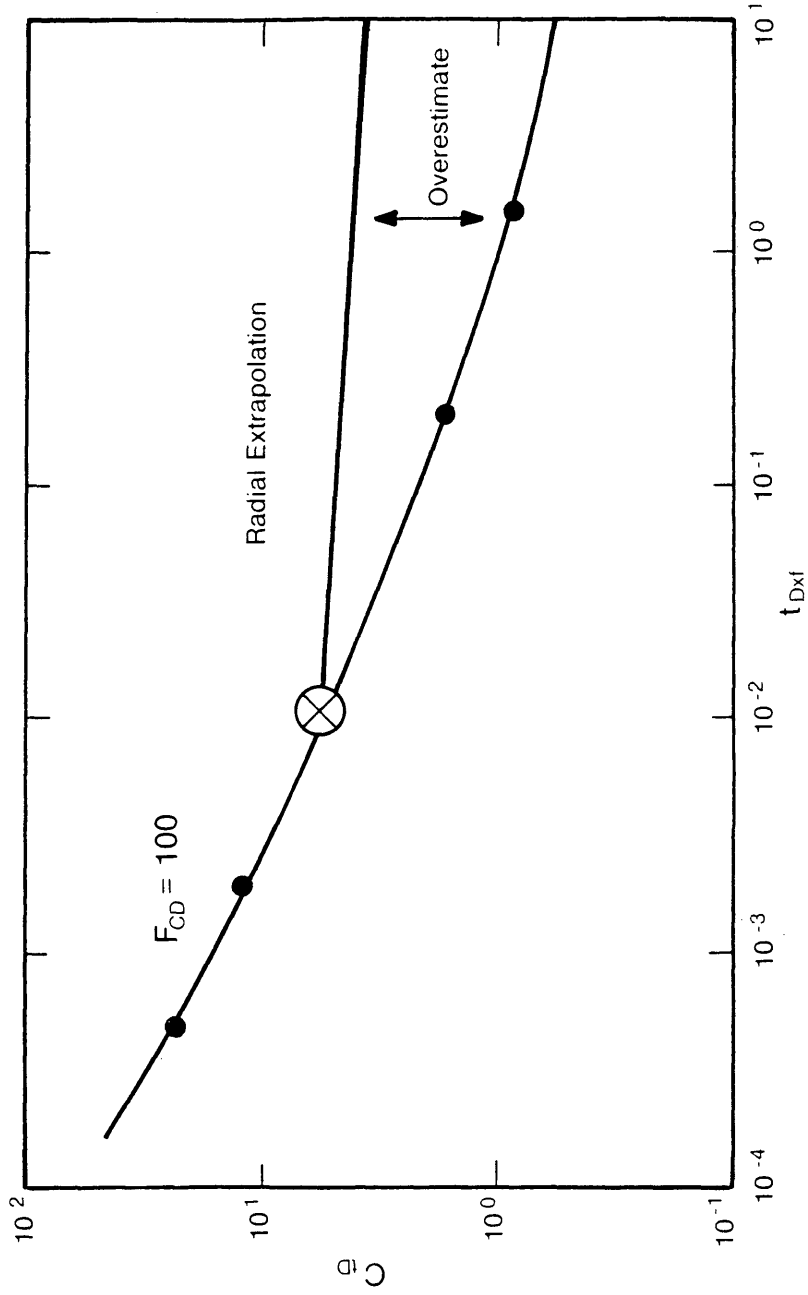


Figure 27. Radial Flow Extrapolation to Determine the Stabilized Performance Coefficient for a Finite Conductivity Vertically Fractured Gas Well

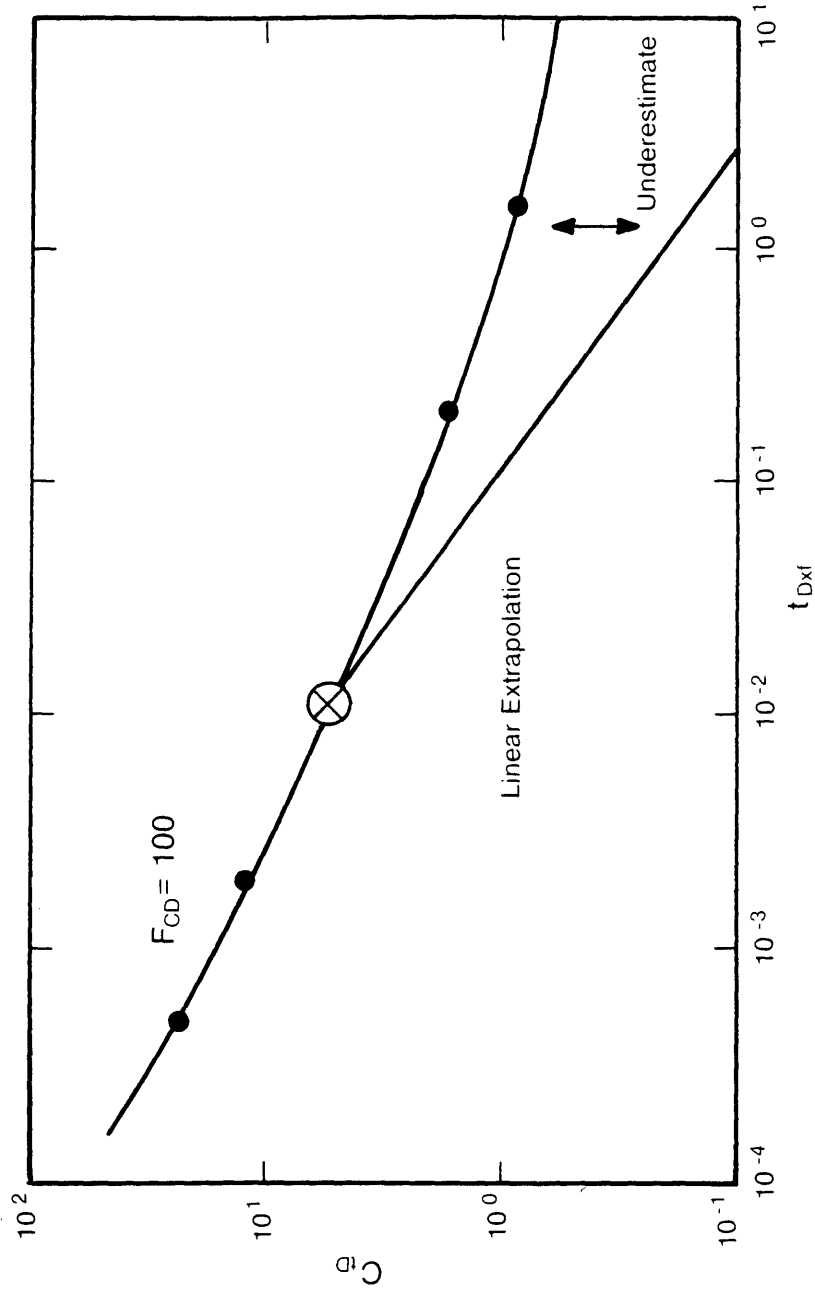
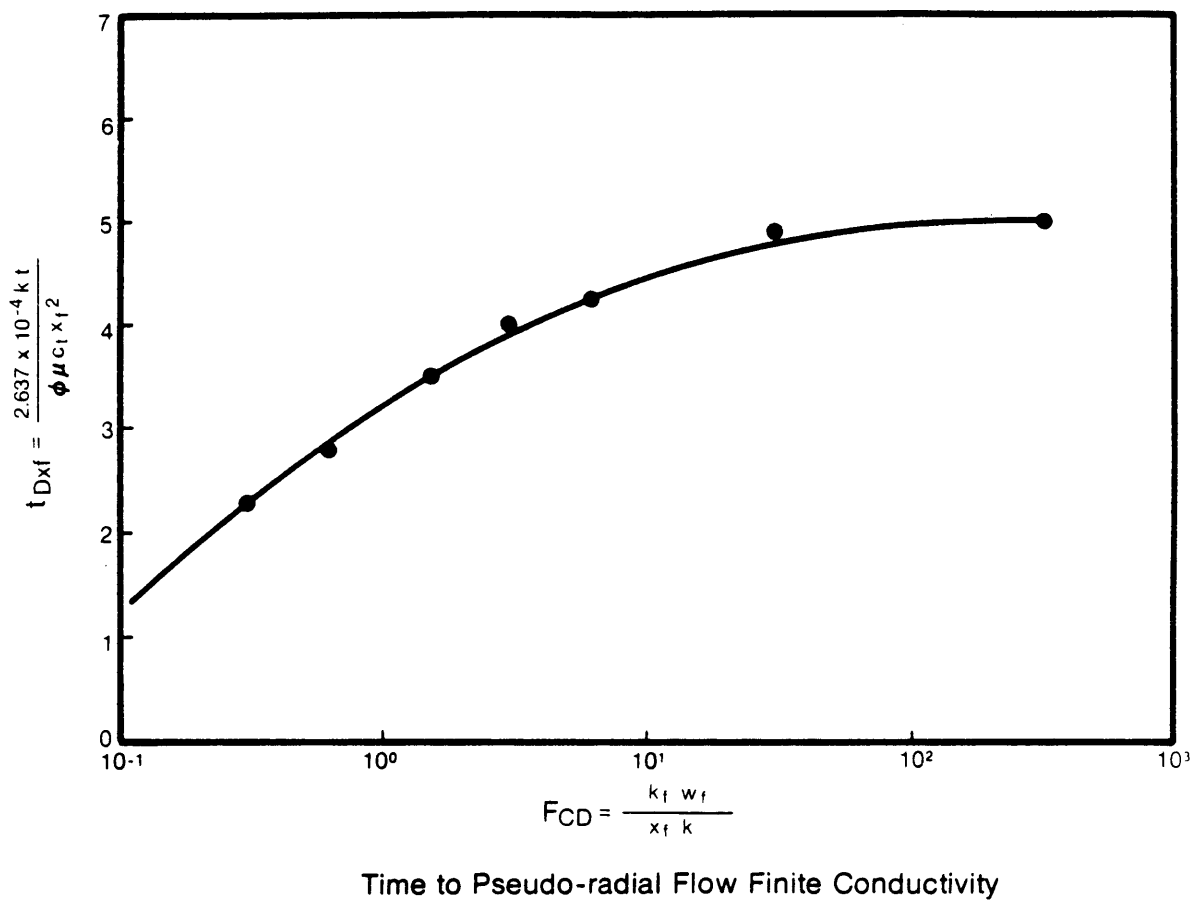


Figure 28. Linear Flow Extrapolation to Determine the Stabilized Performance Coefficient for a Finite Conductivity Vertically Fractured Gas Well



**Figure 29. Time to Pseudo-Radial Flow for a Finite Conductivity Vertically Fractured Gas Well**

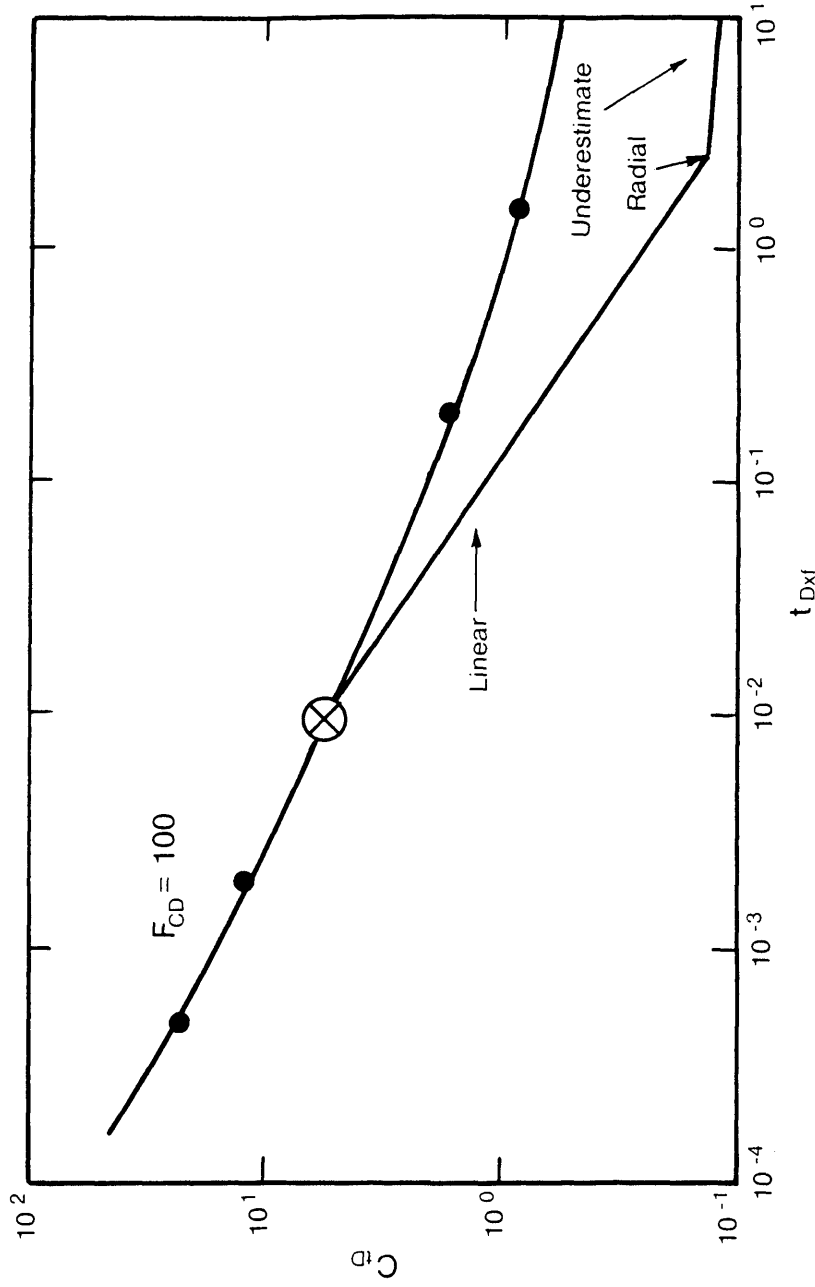


Figure 30. Linear Flow/Radial Flow Extrapolation to Determine the Stabilized Performance Coefficient for a Finite Conductivity Vertically Fractured Gas Well

Determination of the stabilized performance coefficient for a finite conductivity vertically fractured well cannot be accomplished using the standard methods (radial and linear flow assumptions). Knowledge of the reservoir flow condition is necessary.

GENERALIZED STABILIZED DELIVERABILITY

The  $C_t$  determined from the simulation of finite conductivity vertical fractures shows an inverse proportionality to pressure. The inverse relationship of  $C_t$  and pressure can be proved by expressing the backpressure relationship (for  $n = 1$ ) in dimensionless form resulting in:

$$C_{SD} \text{ or } C_{t_D} = 1/p_D \quad (9)$$

The derivation of Equation (9) is shown in Appendix B. Figure 31 shows a comparison of  $1/C_{t_D}$  and  $p_D$  for Agarwal et al's finite conductivity type curve (34). The figure shows excellent agreement. The relationship of  $1/C_{t_D}$  and  $p_D$  provides a way of determining the flow geometry, which is necessary for the proper determination of stabilized performance. Type curves of  $p_D$  are published for many reservoir descriptions. With that knowledge of  $p_D$  the stabilized performance coefficient can be determined.

For example, values of  $C_S$  were calculated by applying Equation (9) for fracture lengths of 100 and 1000 feet, and compared to  $C_S$  determined by simulation of an extended flow period lasting 30 days. Early time (linear and

transitional flow)  $1/C_t$  was matched to a finite conductivity vertical fracture type curve. The match points were used to determine dimensionless fracture conductivity, reservoir permeability, and fracture length. These values were then used to calculate a pseudo-skin factor ( $s_f$ ) (35).

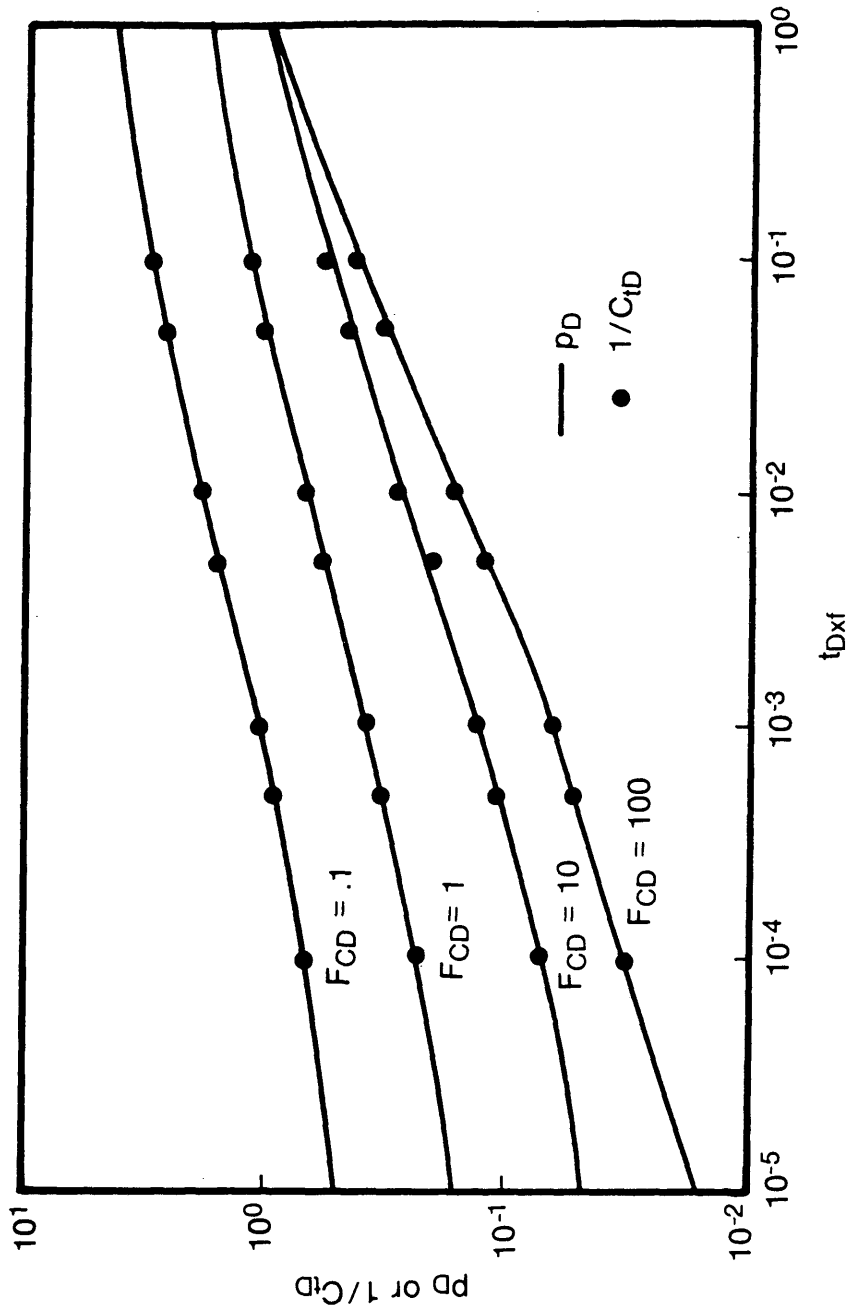


Figure 31. Comparison of 1/CtD and PD for a Finite Conductivity Vertically Fractured Gas Well

The stabilized performance coefficient ( $C_S$ ) was calculated using the pseudosteady state equation where:

$$C_S = \frac{.703 \times 10^{-6} kh}{T \bar{\mu} \bar{z} (\ln r_e/r_w - .75 + s_f)} \quad (10)$$

Excellent agreement is obtained when compared to the simulation results as shown in Figure 32.

As in the previous example, careful measurement of  $1/C_t$  with time can be used in a manner analogous to pressure to determine reservoir properties such as permeability and skin, which then can be used to determine  $C_S$ . As another example, a radial flow simulation was performed, and  $C_t$  measured for 1, 2, 4, 6 and 8 hours of flow. Inverse  $C_t$  was plotted against the log of time and the slope of the line was used to determine  $kh$  and  $s$ , where:

$$kh = \frac{1.632 \times 10^6 \bar{z} \bar{\mu} T}{m} \quad (11)$$

$$s = 1.1513 \left[ \frac{1/C_t (\Delta t = 1 \text{ hr})}{m} - \log \frac{k}{\bar{\phi} \bar{\mu} c r_w^2} + 3.2275 \right] \quad (12)$$

The calculated  $kh$  and  $s$  matched the simulator values. It should be noted that for  $n = 1$ ,  $1/C_t$  is equivalent to " $a_t$ " in the Forchheimer expression.

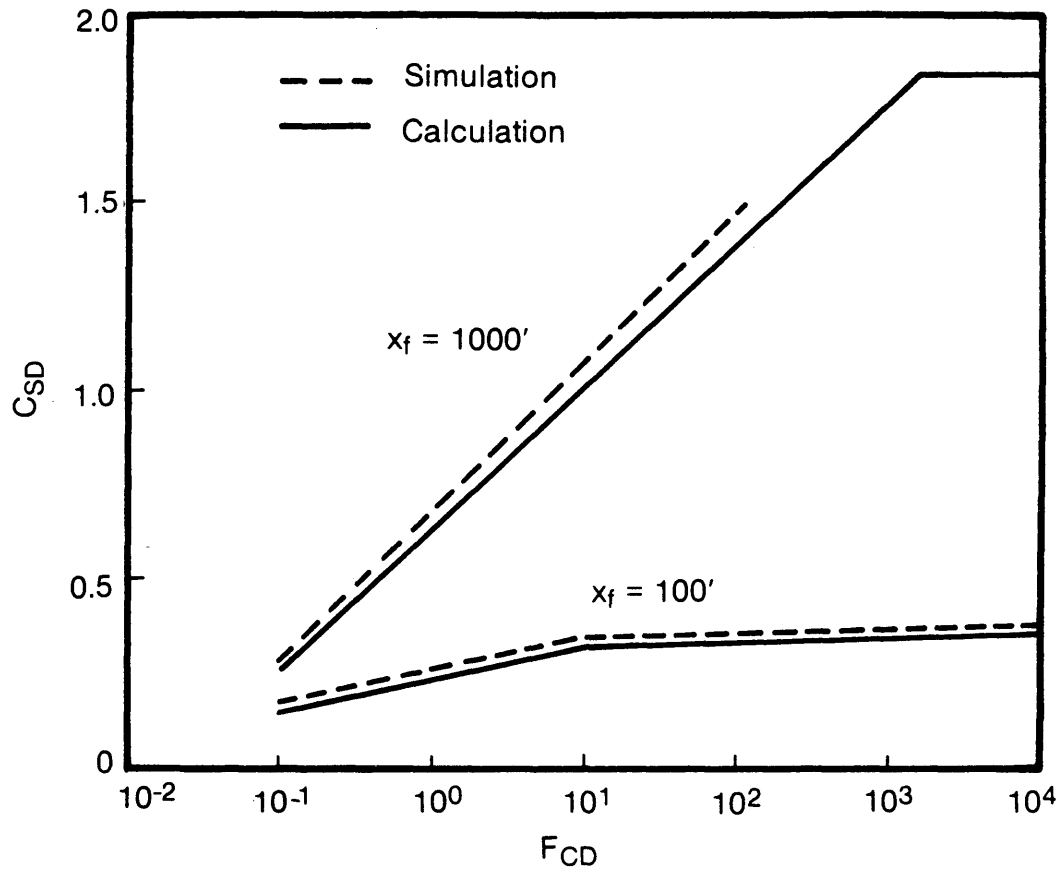


Figure 32. Stabilized Performance Coefficient for a Finite Conductivity Vertically Fractured Gas Well

A similar analysis for radial flow has been made for the case of non-Darcy flow. For "n" not equal to one a plot of  $(1/C_t)^{1/n}$  can be used in a similar manner as described above. The slope of a plot of  $(1/C_t)^{1/n}$  vs  $\log t$  is developed in Appendix C and is shown below:

$$m = 1.632 \times 10^6 \frac{\bar{\mu} \bar{z} T}{kh} Q^* \frac{n-1}{n} \quad (13)$$

Where  $Q^*$  is 1 MMscf/D,  $(1/C_t)^{1/n}$  is the intercept at  $Q$  equal 1 MMscf/D on the performance plot therefore, is analogous to a drawdown test at a rate of 1 MMscf/D. A plot of  $(1/C_t)^{1/n}$  vs  $\log t$  will result in a straight line for which reservoir properties can be determined using equation (11) or the line can be extrapolated to the stabilized performance coefficient.

The stabilized performance coefficient can be determined by extrapolating a plot of  $1/C_t^{1/n}$  vs  $\log t$  to the pseudo stabilization time ( $t_{ps}$ ) where (43):

$$t_{ps} = \frac{376 \phi \bar{\mu} C r_e^2}{k} \quad (14)$$

It may be argued that this is not valid because the Forchheimer equation when plotted as  $\log \Delta P^2$  vs  $\log q$  is not a straight line. However, practical flow rates in

deliverability testing generally are only over one order of magnitude whereas it takes several orders of magnitude change to observe the non-linear behavior of the Forchheimer equation. In other words, short segments of the Forchheimer plot can be represented as straight lines on a  $\log \Delta P^2$  vs  $\log q$  plot, as is the case in deliverability testing.

A number of isochronal and modified isochronal test data were plotted in this manner, and in all cases the plots resulted in straight lines for  $1/C_t^{1/n}$  vs  $\log t$ . In addition, the procedure was verified by rigorous application of the Forchheimer equation. The Forchheimer equation was used to generate pressures to be analyzed using the Rawlins and Schellhardt back pressure expression. Large variations in flow rate, flow time, and reservoir properties were studied. In all cases a plot of  $1/C_t^{1/n}$  vs  $\log t$  resulted in a straight line. The slope of the line was able to reproduce the reservoir properties input if calculated for a constant rate of 1 MMCFD.

As an example, Figure 34 shows a plot of  $1/C_t^{1/n}$  versus  $\log t$  for a long term flow test from Cullender's paper, Gas Well No. 3 (2).

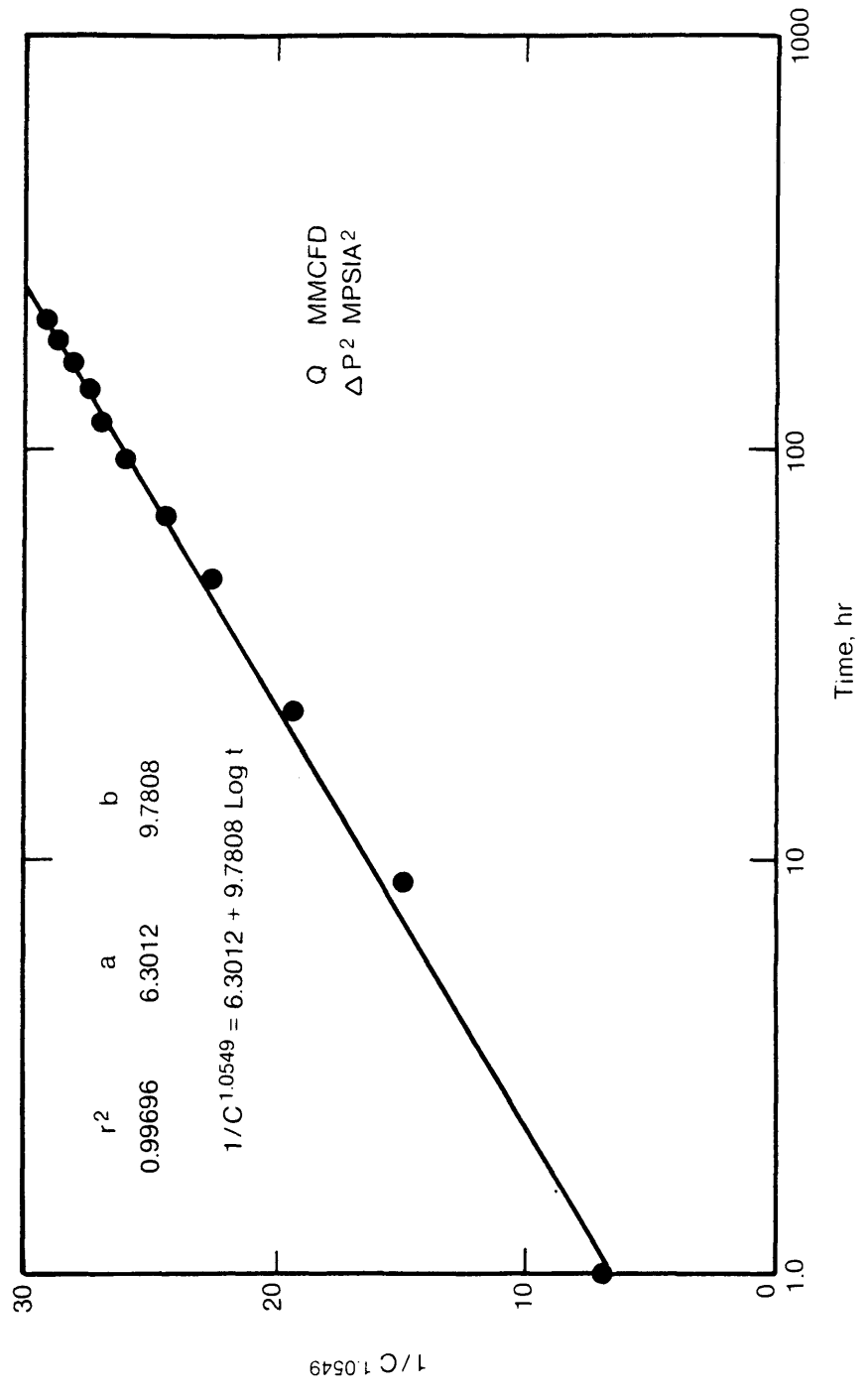


Figure 33.  $(1/C_t)^{1/n}$  vs Log Time (Cullender)

EFFECTS OF WELLBORE STORAGE ON BACKPRESSURE TESTS

The effect of WBS (or afterflow) on a backpressure test has been evaluated by correcting for the true sand face flow rate;

$$q_{sf} = q_{sc} \left[ 1 - C_D \frac{dp_D(t_D, C_D)}{dt_D} \right] \quad (14)$$

$$\frac{q_{sf}}{q_{sc}} = 1 - C_D \frac{dp_D}{dt_D}(t_D, C_D) \quad (15)$$

This analysis assumes, among other things, that friction losses are negligible or are constant.

Proper interpretation of the measured flowing bottom-hole pressure during a flow period can be made by multiplying the surface measured flow rate by Equation (14).

$$\left[ 1 - C_D \frac{dp_D(t_D, C_D)}{dt_D} \right] q_{sc} = C (P_i^2 - P_{wf}^2)^n \quad (16)$$

Evaluation of the derivative term in Equation (16) is given by Agarwal, et al (37).

for short time

$$C_D \frac{dp_D(t_D, C_D, s)}{dt_D} = 1 - \frac{2}{C_D} \sqrt{\frac{t_D}{\pi}} + \frac{t_D}{C_D} \left( \frac{1}{C_D} - \frac{1}{2} \right) \quad (17)$$

for long time

$$C_D \frac{dp_D(t_D, C_D, s)}{dt_D} = - [P_D(t_D) + s] \left[ C_D \left( \frac{1 - 2 C_D}{2 t_D^2} \right) \right] + \frac{C_D}{2 t_D^2} [t_D - C_D + s] \quad (18)$$

Given closer study it is clear that for constant time, the variation in sandface flow is dependent upon wellbore compressibility. For cases with small variation in wellbore compressibility, the performance plot will be shifted to the right by a constant amount. The slope on a performance plot (or flow exponent) will not be in error. However, if drawdowns are large, wellbore compressibility may vary significantly causing greater adjustment in sandface flow for higher rates (larger drawdown). This will result in a reduced slope (or overestimated flow exponent) on the performance plot (Figure 34). WBS will lead to an erroneous

interpretation and a significant overestimate in AOF.

It is recommended that backpressure tests be of sufficient duration to minimize the influence of after flow. As a rule, flow time should be greater than (38):

$$t_{\text{WBS}} \gtrsim 60 C_D + s \quad (19)$$

### CONCLUSIONS

1. Stabilized flow-after-flow and isochronal tests are valid.
2. Because in most instances flow-after-flow tests are not stabilized (i.e., do not reach pseudosteady-state), they have error caused by continued influence of previous flow periods. The flow exponent, "n", is underestimated, and the performance coefficient is not representative of the stabilized value. These errors do not permit a reliable estimate of well deliverability.
3. Modified isochronal tests have superposition error. However, for the modified isochronal test, with equal flow and shut-in periods, the error in "n" is 1/3 as great as that for the unstabilized flow-after-flow test with an equivalent flow period. The superposition error associated with the modified isochronal test can be reduced by decreasing the flow rate ratios, and use a normal flow sequence. Furthermore, typical modified isochronal tests use equal flow and equal shut-in times. This is not a necessary requirement. In fact, error in "n" can be reduced significantly for flow time to shut-in time ratios less than one.

4. Isochronal and modified isochronal tests provide transient deliverability. An extended flow test or a computational method of estimating the stabilized deliverability is necessary. Most methods for predicting stabilized deliverability from transient deliverability assume a radial flow geometry. Applying this flow assumption for a well having a finite conductivity vertical fracture will result in an overestimate of stabilized deliverability. Similarly, a linear flow assumption will cause an underestimate of deliverability. The presence of finite conductivity fractures does not affect the flow exponent "n".
5. For Darcy flow the performance coefficient is inversely related to the pressure time function for the reservoir. The inverse performance coefficient can be used to determine reservoir properties in a manner analogous to pressure. For isochronal tests with a non-Darcy flow contribution  $(1/C_t)^{1/n}$  can be used in a manner similar to pressure to determine reservoir properties. The stabilized performance coefficient can be determined by extrapolating a plot of  $(1/C_t)^{1/n}$  vs  $\log t$  to a time  $t$  equal to  $t_{ps}$ .

6. For small wellbore compressibility, WBS will shift the performance plot, but will not affect the flow exponent. For large drawdown, wellbore compressibility is likely to change significantly during each flow period. In this case, WBS will cause a reduction in slope on the performance plot. These errors will cause a significant overestimate of AOF. It is recommended that flow times used in backpressure tests be greater than the time required for WBS effects to dissipate.

RECOMMENDATIONS FOR FUTURE RESEARCH

Further study should be given to the cause and effect of non-Darcy flow on well flow behavior. It is this author's opinion that most non-Darcy Flow will occur in the completion. Little attention has been given to non-Darcy Flow in the well completion and much may be learned.

It is further recommended that this work be carried on to provide correction curves for backpressure tests influenced by superposition error and non-Darcy effects.

It is also recommended that study be given to the effect of WBS considering a more rigorous approach than attempted in this work. Factors which may be included are frictional pressure loss variation, backpressure through a restrictive choke and etc.

ARTHUR LAKES LIBRARY  
COLORADO SCHOOL of MINES  
GOLDEN, COLORADO 80401

NOMENCLATURE

a	=	coefficient of flow q, psia <sup>2</sup> /MMscf/D
a <sub>t</sub>	=	transient value of a, psia <sup>2</sup> /MMscf/D
b	=	coefficient of flow q <sup>2</sup> , psia/(MMscf/D) <sup>2</sup>
C <sub>w</sub>	=	wellbore compressibility (psi <sup>-1</sup> )
$\bar{c}$	=	average gas compressibility, (psi <sup>-1</sup> )
C <sub>D</sub>	=	dimensionless WBS $V_{ws}C_{ws}/\phi hcr_w^2$
C <sub>tD</sub> or C <sub>SD</sub>	=	dimensionless performance coefficient =
		$\frac{1.422 \times 10^6 \bar{\mu} \bar{z} T}{kh} (C_t \text{ or } C_s)$
C <sub>s</sub>	=	stabilized performance coefficient, MMscf/D/psia <sup>2</sup>
C <sub>t</sub>	=	transient performance coefficient, MMscf/D/psia <sup>2</sup>
D	=	Non-Darcy Flow turbulence factor.
F <sub>CD</sub>	=	dimensionless fracture conductivity = $\frac{k_f w_f}{k x_f}$
h	=	formation thickness, ft
k	=	formation permeability, md
k <sub>f</sub>	=	fracture permeability, md
m	=	semi-log slope, MMscf/D/psia/cycle
M <sub>BP</sub>	=	slope of backpressure curve
$\Delta M$ BP	=	relative slope deviation of backpressure curve caused by superposition error

- $n$  = flow exponent (inverse slope of backpressure curve,  $1/M_{BP}$ )
- $p_B$  = pressure base, psia
- $p_D$  = dimensionless pressure =  $\frac{p_i^2 - p_{wf}^2}{p_i^2 q_D}$
- $\bar{p}_R$  = static reservoir pressure, psia
- $p_s$  = shut-in pressure, psia
- $p_{wf}$  = flowing well pressure, psia
- $q_{sc}$  = flow rate, MMscf/D
- $q_D$  = dimensionless flow rate =  $\frac{1.422 \times 10^6 \bar{\mu} \bar{z} T q_{sc}}{kh p_i^2}$
- $Q^*$  = flow rate for drawdown evaluation only  
 $(1/C_t)^{1/n}$ , MMscf/D
- $r_e$  = drainage radius, ft
- $r_D$  = dimensionless radius =  $r/r_w$
- $r_w$  = wellbore radius, ft
- $s$  = skin
- $s_f$  = pseudo-skin for finite conductivity vertical fractures
- $t_f$  = flow time, hrs

$t_{ps}$	= pseudo-stabilization time, $\frac{376\bar{\phi}\bar{\mu}cr_e^2}{k}$
$t_s$	= shut-in time, hrs
$t_D$	= dimensionless flow time = $\frac{2.637 \times 10^{-4} kt_f}{\bar{\phi} \bar{\mu} \bar{c} r_w^2}$
$t_{DXf}$	= dimensionless flow time = (fractured well) $\frac{2.637 \times 10^{-4} kt_f}{\bar{\phi} \bar{\mu} \bar{c} x_f^2}$
$t_{WBS}$	= end of WBS, hrs
$T$	= reservoir temperature, °R
$T_B$	= temperature base, °F
$T_{res}$	= reservoir temperature, °F
$V_{WS}$	= wellbore volume bbls
$\bar{\mu}$	= average gas viscosity, cp
$w_f$	= fracture width, ft
$x_f$	= fracture half length, ft
$\bar{z}$	= average gas compressibility
$\phi$	= porosity

### REFERENCES

1. Rawlins, E. L., and Schellhardt, M. A.: "Back-Pressure Data on Natural Gas Wells and Their Application to Production Practices", U. S. Bureau of Mines Monograph 7, (1936).
2. Cullender, M. H.: "The Isochronal Performance Method of Determining the Flow Characteristics of Gas Wells", Trans. AIME (1955), Vol. 204, 137.
3. Ferguson, J. W.: "Calculation of Back-Pressure Tests on Natural Gas Wells", Oil and Gas Journal (January 19, 1939).
4. "Methods of Determining Gas Well Capacities in the Panhandle Field from Back Pressure Data", Engineering Department, Oil and Gas Division, Texas Railroad Commission (June 1, 1939).
5. Haymaker, E. R., Binckley, C. W., and Burgess, F. R.: "Method of Establishing a Stabilized Back Pressure Curve for Gas Wells Producing from a Reservoir of Extremely Low Permeability", Trans. AIME (1942) Vol. 146, 166.
6. Ikoku, C. U.: Natural Gas Engineering, A Systems Approach, PennWell Books, Tulsa (1980) pp. 356-414.

7. Baumel, J. K., and Breitung, C. A.: "Back Pressure Test for Natural Gas Wells, State of Texas", Railroad Commission of Texas (July 31, 1950).
8. Katz, D. L., Varg, J. A., and Elenbaas, J. R.: "Design of Gas Storage Fields", Trans. AIME (1959), Vol. 216, 11.
9. Miller, J. S., Walker, C. J., and Danning H. N.: "Productivity Tests on a Large-Capacity Gas Well", The Petroleum Engineer (February 1959), pp. B-23 - B-26.
10. Graham, J. R. and Boyd, W. E.: "An Analysis of Changing Backpressure Test Curves from Some Gulf Coast Area Gas Wells", Journal of Petroleum Technology (December 1987), pp. 1541-1546.
11. Aziz, K.: "Theoretical Basis of Isochronal and Modified Isochronal Back-Pressure Testing of Gas Wells", J. Can. Pet. Tech. 6 (1), pp. 20-22.
12. Mattar, L., Fekete, T., and Lin, C.: "Validity of Isochronal and Modified Isochronal Testing of Gas Wells", paper SPE 10126 presented at the 1981 SPE-AIME Annual Fall Technical Conference, San Antonio (Oct. 5-7, 1981).
13. Houpeurt, A.: "Analogy of Radial Circular Transient Flow of Gases in Porous Media", Rev. Inst. Franc.

- petrole et Ann, combustibles liquide (1953) 8 (4) 129,  
8 (5): 193; 8 (6): 248.
14. Houpeurt, A.: "Mouvements des Fluides Dans Les  
Gisements D'Hydrocarbures; Essai des Puits, Production  
Tome III", Institut Francais du Petrole (1958) 85.
15. Forchheimer, P.: "Wasserbewegung durch Boden", Zeit  
der Deutsch Ing. 45 (1901) pp. 1731.
16. Katz, D. L., Cornell, D., Kobayashi, R., Poettmann,  
F. H., Vary, J. A., Elenbaas, J. R., and Weinaug, C.  
F.: Handbook of Natural Gas Engineering, McGraw-Hill,  
New York (1959).
17. Cornell, D.: "Unsteady State Flow in Gas Reservoirs",  
World Oil, Vol. 144, No. 2 (February 1, 1957) pp. 133-  
134.
18. Cornell, D.: "Calculations of Stabilized Gas Well  
Performance Curves From Backpressure Test Data",  
Trans. AIME (1955) 204, 255.
19. Tek, M. F., Grove, M. L., and Poettmann, F. H.:  
"Method for Predicting the Backpressure Behavior of  
Low Permeability Natural Gas Wells", Trans. AIME  
(1957) 210, 302.

20. Poettmann, F. H., and Schilson, R. E.: "Calculation of the Stabilized Performance Coefficient of Low Permeability Natural Gas Wells", Trans. AIME (1959) 216, 240.
21. Rodgers, J. S., and Pasad, R. K.: "Effects of Drainage Shape and Well Location on Stabilized Gas Deliverability Calculations", paper SPE 3836 presented at the 1972 SPE-AIME Rocky Mountain Regional Meeting, Denver, Co. (April 10-13, 1972).
22. Carter, R. D., Miller, S. C., Jr., and Riley, H. G.: "Determination of Stabilized Gas Well Performance from Short Flow Tests", Trans. AIME (1963) 230, 651-658.
23. Hadinoto, N., Raghavan, R., and Thomas, G. W.: "Determination of Gas Well Deliverability of Vertically Fractured Wells", paper SPE 6136 presented at the 1976 SPE-AIME 51st Annual Fall Technical Conference, New Orleans, (Oct., 3-6).
24. Hadinoto, N.: Determination of Gas Well Deliverability in Vertically Fractured Wells, M. S. Thesis, Tulsa University (1975).
25. Tariq,, M. S.: Effect of Vertical Fractures on Back Pressure Test Behavior of Gas Wells, M. S. Thesis, Stanford University (1975).

26. Brar, G. S., and Aziz, K.: "The Analysis of Modified Isochronal Tests to Predict Stabilized Deliverability Potential of Gas Wells Without Using Stabilized Flow Data", J. Pet. Tech. (Feb., 1978) pp. 297-304.
27. Poettmann, F. H.: "Discussion of Analysis of Modified Isochronal Tests to Predict Stabilized Deliverability Potential of Gas Wells Without Stabilized Flow Data", J. Pet. Tech. (Oct., 1986), pp. 1122-1124.
28. Prats, M., Hazebroek, P., and Strickler, W. R.: "Effect of Vertical Fractures on Transient Pressure Behavior-Compressible-Fluid Case", Soc. Pet. Eng. J. (June, 1962) pp. 87-94.
29. Russell, D. G., and Truitt, N. E.: "Transient Pressure Behavior in Vertically Fractured Reservoirs", J. Pet. Tech. (Oct., 1964) 1159-1170.
30. Millheim, K. K., and Cichowicz, L.: "Testing and Analyzing Low Permeability Fractured Gas Wells", J. Pet. Tech. (Feb., 1968) 193-198.
31. Wattenbarger, R. A., and Ramey, H. J., Jr.: "Well Test Interpretation of Vertically Fractured Gas Wells", J. Pet. Tech., (May, 1969) 625-632.
32. Eilerts, C.: "Methods for Estimating Deliverability After Massive Fracture Completions in Tight Formations", paper SPE 5112 presented at the 1974 Deep

- Drilling and Production Symposium, Amarillo, Tx. (Sept. 8-10, 1974).
33. Gringarten, A. C., Ramey, H. J., Jr., Raghaven, R.: "Applied Pressure Analysis for Fractured Wells", Soc. Pet. Eng. J. (July, 1975) 887-892.
  34. Agarwal, R. G., Carter, R. D., and Pollock, C. B.: "Evaluation and Prediction of Performance of Low Permeability Gas Wells Stimulated By Massive Hydraulic Fracturing", paper SPE 6838 presented at the 1977 SPE AIME 52nd Annual Fall Technical Conference, Denver, Co. (Oct. 9-12, 1977).
  35. Cinco-Ley, H. L., Samaniego, F. V., and Dominguez, N. A.: "Transient Pressure Behavior For A Well With Finite Conductivity Vertical Fracture", Soc. Pet. Eng. J. (Aug., 1978) 253-264.
  36. Sinha, M. K., and Furlong, K. D.: "Gas Well Deliverability Prediction-For Hydraulically Fractured (Vertical) Wells in Tight Reservoirs", paper SPE 7948 presented at the 1979 Symposium on Low Permeability Gas Reservoir, Denver, Co. (May 20-22, 1979).
  37. Agarwal, R. G., Al-Hussainy, R., and Ramey, H. J., Jr.: "An Investigation of Wellbore Storage and Skin Effect in Unsteady Liquid Flow: I Analytical Treatment", Soc. Pet. Engr. J. (Sept., 1970) 279-289.

38. Earlougher, R. C., Jr.: Advances in Well Test Analysis, Soc. of Pet. Engr. of AIME, New York (1977) pp. 10-11.
39. Al-Hussainy, R., Ramey, H. J., Jr., and Crawford, P. B.: "The Flow of Real Gases Through Porous Media", J. Pet. Tech. (May, 1966) 624-636.
40. Al-Hussainy, R., and Ramey, H. J., Jr.: "Application of Real Gas Flow Theory to Well Testing and Deliverability Forecasting", J. Pet. Tech. (May 1966) 637-642.
41. Fetkovich, M. J.: "Multipoint Testing of Gas Wells", Continuing Education Course No. 9, SPE Mid-Continent Section, March 1975.
42. Bass, D. M., Jr.: A Study of The Factors Which Affect The Results of Short-Term Multi-Rate Gas Well Tests, PhD. Dissertation, Texas A&M University (1971).
43. Hinchman, S. B., Kazemi, H., and Poettmann, F. H.: "Further Discussion of the Analysis of Modified Isochronal Tests to Predict the Stabilized Deliverability of Gas Wells Without Using Stabilized Flow Data", J. Pet. Tech. (Jan. 1987) pp. 93-96.

APPENDIX A

The principle of superposition has been used to determine the validity of flow-after-flow, isochronal, and modified isochronal tests. The diffusivity equation is a linear differential equation. As used here, the superposition principle states that adding solutions to a linear differential equation results in a new solution to that differential equation.

$$\Delta p = \Delta p_a + \Delta p_b + \dots \quad (\text{A-1})$$

A flow-after-flow test which reaches Pseudosteady-state for each flow period can express the pressure difference squared for each flow period as:

$$\begin{aligned} (\bar{p}_R^2 - p_{wf}^2)_1 &= q_{D1} \bar{p}_R^2 (\ln r_D - .75 + s) \\ (\bar{p}_R^2 - p_{wf}^2)_2 &= q_{D2} \bar{p}_R^2 (\ln r_D - .75 + s) \\ (\bar{p}_R^2 - p_{wf}^2)_3 &= q_{D3} \bar{p}_R^2 (\ln r_D - .75 + s) \\ (\bar{p}_R^2 - p_{wf}^2)_4 &= q_{D4} \bar{p}_R^2 (\ln r_D - .75 + s) \end{aligned} \quad (\text{A-2})$$

and is equivalent to:

$$(\bar{p}_R^2 - p_{wf}^2)_J = \bar{p}_R^2 (\ln r_D - .75 + s) q_{DJ} \quad (\text{A-3})$$

where  $\bar{p}_R^{-2} (\ln r_D - .75 + s)$  is a constant. The slope of the Rawlins and Schellhardt backpressure is determined by:

$$\begin{aligned}
 M_{BP} &= \frac{\log \frac{(\bar{p}_R^{-2} - p_{wf}^2)_J}{(\bar{p}_R^{-2} - p_{wf}^2)_{J-1}}}{\log q_{sc_J} / q_{sc_{J-1}}} \\
 &= \frac{\log (\text{constant } q_{sc_J}) / (\text{constant } q_{sc_{J-1}})}{\log q_{sc_J} / q_{sc_{J-1}}} \\
 &= 1 \qquad \qquad \qquad (A-4)
 \end{aligned}$$

A unit slope for a stabilized flow-after-flow test demonstrates its validity.

The squared pressure difference for a flow-after-flow test which does not reach Pseudosteady-state is rigorously determined using the principle of superposition where:

$$\begin{aligned}
 (\bar{p}_R^{-2} - p_{wf}^2)_1 &= q_{D1} \bar{p}_R^{-2} \left(\frac{1}{2}\right) (\ln t_D + .8097 + s) \\
 (\bar{p}_R^{-2} - p_{wf}^2)_2 &= q_{D2} \bar{p}_R^{-2} \left(\frac{1}{2}\right) (\ln t_D + .8097 + s) \\
 &\quad + q_{D1} \bar{p}_R^{-2} \left(\frac{1}{2}\right) \ln (2) \\
 (\bar{p}_R^{-2} - p_{wf}^2)_3 &= q_{D3} \bar{p}_R^{-2} \left(\frac{1}{2}\right) (\ln t_D + .8097 + s) \\
 &\quad + q_{D2} \bar{p}_R^{-2} \left(\frac{1}{2}\right) \ln (2)
 \end{aligned}$$

$$\begin{aligned}
& + q_{D1} \bar{p}_R^{-2} \left(\frac{1}{2}\right) \ln \left(\frac{3}{2}\right) \\
(\bar{p}_R^2 - p_{wf}^2)_4 & = q_{D4} \bar{p}_R^{-2} \left(\frac{1}{2}\right) (\ln t_D + .8097 + s) \\
& + q_{D3} \bar{p}_R^{-2} \left(\frac{1}{2}\right) \ln (2) \\
& + q_{D2} \bar{p}_R^{-2} \left(\frac{1}{2}\right) \ln \left(\frac{3}{2}\right) \\
& + q_{D1} \bar{p}_R^{-2} \left(\frac{1}{2}\right) \ln \left(\frac{4}{3}\right)
\end{aligned} \tag{A-5}$$

For transient flow  $\bar{p}_R \approx p_i$ .

The slope calculated using flow period 1 and 4 is:

$$\begin{aligned}
M_{BP} & = \frac{\log \left[ (\bar{p}_R^2 - p_{wf}^2)_4 / (\bar{p}_R^2 - p_{wf}^2)_1 \right]}{\log (q_{sc4} / q_{sc1})} \\
& = \log \left\{ \frac{q_{sc4}}{q_{sc1}} + \left[ \frac{\ln \left(\frac{4}{3}\right) + \frac{q_{sc2}}{q_{sc1}} \ln \left(\frac{3}{2}\right) + \frac{q_{sc3}}{q_{sc1}} \ln (2)}{\ln t_D + .8097 + s} \right] \right\} / \log \left( \frac{q_{sc4}}{q_{sc1}} \right)
\end{aligned} \tag{A-6}$$

and the relative error defined as the deviation from the correct slope:

$$\Delta M_{BP} = \frac{\frac{q_{sc1}}{q_{sc4}} \ln \left(\frac{4}{3}\right) + \frac{q_{sc2}}{q_{sc4}} \ln \left(\frac{3}{2}\right) + \frac{q_{sc3}}{q_{sc4}} \ln (2)}{\ln t_D + .8097 + s} \tag{A-7}$$

An isochronal test requires stabilization during each shut-in period; therefore, no superposition of the shut-in periods is necessary. The flow periods are in transient flow, and the squared pressure difference can be expressed as:

$$\begin{aligned} (\bar{p}_R^2 - p_{wf}^2)_1 &= q_{D1} \bar{p}_R^2 \left(\frac{1}{2}\right) (\ln t_D + .8097 + s) \\ (\bar{p}_R^2 - p_{wf}^2)_2 &= q_{D2} \bar{p}_R^2 \left(\frac{1}{2}\right) (\ln t_D + .8097 + s) \\ (\bar{p}_R^2 - p_{wf}^2)_3 &= q_{D3} \bar{p}_R^2 \left(\frac{1}{2}\right) (\ln t_D + .8097 + s) \\ (\bar{p}_R^2 - p_{wf}^2)_4 &= q_{D4} \bar{p}_R^2 \left(\frac{1}{2}\right) (\ln t_D + .8097 + s) \end{aligned} \quad (A-8)$$

and is equivalent to:

$$(\bar{p}_R^2 - p_{wf}^2)_J = \bar{p}_R^2 \left(\frac{1}{2}\right) (\ln t_D + .8097 + s) q_{DJ} \quad (A-9)$$

where  $\bar{p}_R^2 \left(\frac{1}{2}\right) (\ln t_D + .8097 + s)$  is a constant. The slope of the Rawlins and Schellhardt backpressure expression is:

$$M_{BP} = \frac{\log \left[ (\bar{p}_R^2 - p_{wi}^2)_J / (\bar{p}_R^2 - p_{wi}^2)_{J-1} \right]}{\log (q_{scJ} / q_{scJ-1})}$$

$$\begin{aligned}
 &= \frac{\log [(\text{constant } q_{scJ}) / (\text{constant } q_{scJ-1})]}{\log(q_{scJ} / q_{scJ-1})} \\
 &= 1 \qquad \qquad \qquad (A-10)
 \end{aligned}$$

The unit slope demonstrates the validity of an isochronal test.

To properly evaluate a modified isochronal test, the principle of superposition must be applied to the flow and shut-in periods. The squared pressure difference for each flow period then becomes:

$$\begin{aligned}
 (\bar{p}_R^2 - p_{wf1}^2)_1 &= q_{D1} \bar{p}_R^2 \left(\frac{1}{2}\right) (\ln t_D + .8097 + s) \\
 (p_{s1}^2 - p_{wf2}^2)_2 &= q_{D2} \bar{p}_R^2 \left(\frac{1}{2}\right) (\ln t_D + .8097 + s) \\
 &\quad + q_{D1} \bar{p}_R^2 \left(\frac{1}{2}\right) \ln \frac{2(t_f/t_s) + 1}{(t_f/t_s)^2 + 2(t_f/t_s) + 1} \\
 (p_{s2}^2 - p_{wf3}^2)_3 &= q_{D3} \bar{p}_R^2 \left(\frac{1}{2}\right) (\ln t_D + .8097 + s) \\
 &\quad + q_{D2} \bar{p}_R^2 \left(\frac{1}{2}\right) \ln \frac{2(t_f/t_s) + 1}{(t_f/t_s)^2 + 2(t_f/t_s) + 1} \\
 &\quad + q_{D1} \bar{p}_R^2 \left(\frac{1}{2}\right) \ln \frac{3(t_f/t_s)^2 + 8(t_f/t_s) + 4}{4(t_f/t_s)^2 + 8(t_f/t_s) + 4}
 \end{aligned}$$

$$\begin{aligned}
(p_{s_3}^2 - p_{wf_4}^2) &= q_{D4} \bar{p}_R^{-2} \left(\frac{1}{2}\right) (\ln t_D + .8097 + s) \\
&+ q_{D3} \bar{p}_R^{-2} \left(\frac{1}{2}\right) \ln \frac{2(t_f/t_s) + 1}{(t_f/t_s)^2 + 2(t_f/t_s) + 1} \\
&+ q_{D2} \bar{p}_R^{-2} \left(\frac{1}{2}\right) \ln \frac{3(t_f/t_s)^2 + 8(t_f/t_s) + 4}{4(t_f/t_s)^2 + 8(t_f/t_s) + 4} \\
&+ q_{D1} \bar{p}_R^{-2} \left(\frac{1}{2}\right) \ln \frac{8(t_f/t_s)^2 + 18(t_f/t_s) + 9}{9(t_f/t_s)^2 + 18(t_f/t_s) + 9}
\end{aligned}
\tag{A-11}$$

where the squared pressure difference is the square of the previous shut-in period pressure ( $p_s$ ) less the square of the flowing pressure ( $p_{wf}$ ) at a specific time ( $t_f$ ). The slope calculated using flow period 1 and 4 is:

$$\begin{aligned}
M_{BP} &= \frac{\log \left( \frac{p_{s_3}^2 - p_{wf_4}^2}{p_{s_1}^2 - p_{wf_1}^2} \right)}{\log \left( \frac{q_{sc4}}{q_{sc1}} \right)} \\
&= \log \left\{ \frac{q_{sc4}}{q_{sc1}} + \left[ \ln \frac{8(t_f/t_s)^2 + 18(t_f/t_s) + 9}{9(t_f/t_s)^2 + 18(t_f/t_s) + 9} \right. \right. \\
&\quad \left. \left. + \frac{q_{sc2}}{q_{sc1}} \ln \frac{3(t_f/t_s)^2 + 8(t_f/t_s) + 4}{4(t_f/t_s)^2 + 8(t_f/t_s) + 4} \right] \right\}
\end{aligned}$$

$$+ \frac{q_{sc3}}{q_{sc4}} \ln \frac{2(t_f/t_s) + 1}{(t_f/t_s)^2 + 2(t_f/t_s) + 1} \left. \vphantom{\frac{q_{sc3}}{q_{sc4}}} \right\} / (\ln t_D + .8097 + s) / \log \frac{q_{sc4}}{q_{sc9}} \quad (A-12)$$

The maximum relative error defined as the deviation from the correct slope is:

$$\begin{aligned} \Delta M_{BP} = & \left( \frac{q_{sc1}}{q_{sc4}} \ln \frac{8(t_f/t_s)^2 + 18(t_f/t_s) + 9}{9(t_f/t_s)^2 + 18(t_f/t_s) + 9} \right. \\ & + \frac{q_{sc2}}{q_{sc4}} \ln \frac{3(t_f/t_s)^2 + 8(t_f/t_s) + 4}{4(t_f/t_s)^2 + 8(t_f/t_s) + 4} \\ & \left. + \frac{q_{sc3}}{q_{sc4}} \ln \frac{(t_2/t_f) s + 1}{(t_f/t_s)^2 + 2(t_f/t_s) + 1} \right) / (\ln t_D + .8097 + s) \quad (A-13) \end{aligned}$$

For  $t_f = t_s$ :

$$\begin{aligned} \Delta M_{BP} = & \left[ \frac{q_{sc1}}{q_{sc4}} \ln \left( \frac{35}{36} \right) + \frac{q_{sc2}}{q_{sc4}} \ln \left( \frac{15}{16} \right) \right. \\ & \left. + \frac{q_{sc3}}{q_{sc4}} \ln \left( \frac{3}{4} \right) \right] / (\ln t_D + .8097 + s) \quad (A-14) \end{aligned}$$

**APPENDIX B**

Using the following dimensionless term definitions, a dimensionless Rawlins and Schellhardt backpressure expression can be derived:

$$q_D = \frac{1.422 \times 10^6 \bar{\mu} \bar{z} T q_{sc}}{khPR^2} \quad (B-1)$$

$$\Delta p_D = \frac{\bar{p}_R^2 - p_{wf}^2}{\bar{p}_R^2 q_D} \quad (B-2)$$

Solving equation (B-1) for  $q_{sc}$  and equation (B-2) for

$(\bar{p}_R^2 - p_{wf}^2)$  results in:

$$q_{sc} = \frac{q_D kh p_i^2}{1.422 \times 10^6 \bar{\mu} \bar{z} T} \quad (B-3)$$

$$\bar{p}_R^2 - p_{wf}^2 = p_i^2 \Delta p_D q_D \quad (B-4)$$

Substitution of equation (B-3) and (B-4) into the backpressure expression (Equation 1), where  $n = 1$  yields;

$$\frac{kh}{1.422 \times 10^6 \bar{\mu} \bar{z} T} = C (t \text{ or } s) \Delta p_D \quad (B-5)$$

If we define a dimensionless performance coefficient ( $C_D$ ) as;

$$C_{t_D} \text{ or } C_{s_D} = \frac{1.422 \times 10^6 \bar{\mu} \bar{z} T}{kh} C_{(t \text{ or } s)} \quad (\text{B-6})$$

Then the backpressure expression becomes:

$$(C_{t_D} \text{ or } C_{s_D}) \Delta p_D = 1$$

or

$$(C_{t_D} \text{ or } C_{s_D}) = 1/p_D \quad (\text{B-7})$$

**APPENDIX C**

The Forchheimer expression

$$\bar{p}_R^2 - p_{wf}^2 = a_t q_{sc} + b q_{sc}^2 \quad (C-1)$$

can be set equal to the Rawlins and Schellhardt expression

$$\bar{p}_R^2 - p_{wf}^2 = (1/c)^{1/n} q_{sc}^{1/n} \quad (C-2)$$

resulting in

$$a_t q_{sc} + b q_{sc} = (1/c)^{1/n} q_{sc}^{1/n} \quad (C-3)$$

Where

$$a_t = 1.631 \times 10^6 \frac{\bar{\mu} \bar{z} T}{kh} \log t_D$$

$$+ 1.140 \times 10^6 \frac{\bar{\mu} \bar{z} T}{kh} + 1.417 \times 10^6 \frac{\bar{\mu} \bar{z} T}{kh} s \quad (C-4)$$

and

$$b = 1.417 \times 10^6 \frac{\bar{\mu} \bar{z} T}{kh} D \quad (C-5)$$

substituting  $a_t$  and  $b$  into equation (C-3) and solving for  $(1/c)^{1/n}$  results in

$$\begin{aligned}
(1/C)^{1/n} & [= 1.631 \times 10^6 \frac{\bar{\mu}\bar{z}\bar{T}}{kh} \log t_D \\
& + 1.146 \times 10^6 \frac{\bar{\mu}\bar{z}\bar{T}}{kh} \\
& + 1.417 \times 10^6 \frac{\bar{\mu}\bar{z}\bar{T}}{kh} s] Q^* \left(\frac{n-1}{n}\right) \\
& + 1.471 \times 10^6 \frac{\bar{\mu}\bar{z}\bar{T}}{kh} D Q^* \left(\frac{2n-1}{n}\right)
\end{aligned} \tag{C-6}$$

A plot of  $(1/C)^{1/n}$  vs  $\log t$  results in a slope.

$$m = 1.631 \times 10^6 \frac{\bar{\mu}\bar{z}\bar{T}}{kh} Q^* \left(\frac{n-1}{n}\right) \tag{C-7}$$